



## Northeast Greenland: ice-free shelf edge at 79.4°N around the Last Glacial Maximum 25.5–17.5 ka

TINE L. RASMUSSEN , CHRISTOF PEARCE, KATRINE JUUL ANDRESEN, TOVE NIELSEN AND MARIT-SOLVEIG SEIDENKRANTZ

BOREAS



Rasmussen, T. L., Pearce, C., Andresen, K. J., Nielsen, T. & Seidenkrantz, M.-S. 2022 (October): Northeast Greenland: ice-free shelf edge at 79.4°N around the Last Glacial Maximum 25.5–17.5 ka. *Boreas*, Vol. 51, pp. 759–775. <https://doi.org/10.1111/bor.12593>. ISSN 0300-9483.

The size of the last glacial ice sheet on the Northeast (NE) Greenland shelf and its interaction with ocean circulation have been the subject of debate. Here we provide insights into the extent of the ice sheet around the Last Glacial Maximum (LGM) and investigate timing and strength of changes in the flow of Atlantic Water. The study is based on a multiproxy investigation of a marine sediment core, gravity core DA17-NG-ST01-019G, from 323-m water depth at the NE Greenland shelf edge at 79.4°N. We present benthic and planktic foraminiferal distribution data, AMS-<sup>14</sup>C dates, sedimentological (ice-rafted debris (IRD) and grain sizes), and geochemical (XRF) data in combination with geophysical (sub-bottom profiler) data. The oldest sediments at the study site are dated to 25.5–17.5 ka, encompassing the time frame from the beginning of the LGM to the early deglaciation. This part is overlain by sediments from the late deglaciation and Holocene. The deposits dating from the LGM are very rich in both planktic and benthic foraminifera and microfossils of excellent preservation. The faunas show that the site generally was affected by a strong flow of relatively warm subsurface Atlantic Water during the LGM and Early Holocene. Conditions turned more polar with cold bottom water flow in the Middle–Late Holocene (c. 7.5 ka to Recent) with presence of mainly agglutinated benthic foraminiferal species. Our data from the LGM also indicate that the deposits were mixed by iceberg scouring, confirmed by the geophysical data showing extensive ploughing of the sediments on the outer shelf area. The results further indicate that the Greenland Ice Sheet did not reach to the edge of the NE Greenland shelf at 79.4°N during the LGM 24–18 ka.

*Tine L. Rasmussen (tine.rasmussen@uit.no), Centre for Arctic Gas Hydrate, Environment and Climate, Department of Geosciences, UiT the Arctic University of Norway, Dramsveien 201, 9037 Tromsø, Norway; Christof Pearce and Marit-Solveig Seidenkrantz, Paleocceanography and Paleoclimate Group, Department of Geoscience, Aarhus University, Høegh-Guldbergs Gade 2, DK-8000 Aarhus, Denmark and Arctic Research Centre, Aarhus University, DK-8000 Aarhus, Denmark and iClimate Centre, Aarhus University, DK-8000 Aarhus, Denmark; Katrine Juul Andresen, SeisLab, Department of Geoscience, Aarhus University, Høegh-Guldbergs Gade 2, DK-8000 Aarhus, Denmark; Tove Nielsen, Geological Survey of Denmark and Greenland GEUS, Øster Voldgade 10, 1350 Copenhagen K, Denmark; received 24th November 2021, accepted 22nd April 2022.*

The Greenland Ice Sheet is melting rapidly losing more than 200 Gt year<sup>-1</sup> of ice in recent years (Van den Broeke *et al.* 2009; Mouginit *et al.* 2019; Mankoff *et al.* 2021; Simonsen *et al.* 2021) due to increasing global atmospheric temperatures and ocean warming (e.g. Luckman *et al.* 2006; Howat *et al.* 2007; Holland *et al.* 2008; Lindemann *et al.* 2020; Schaffer *et al.* 2020). The southern and western margin of the inland ice reacted first, then further north in the western section (e.g. Howat *et al.* 2007; Van den Broeke *et al.* 2009; Bjørk *et al.* 2012; Rignot & Mouginit 2012; Kjeldsen *et al.* 2015; Mouginit *et al.* 2015; Khan *et al.* 2020). Recently, the large ice streams facing the NE Greenland shelf (e.g. Nioghalvfjærdersfjorden and Zachariae glaciers) have accelerated in melting and calving (Rignot & Mouginit 2012; Mouginit *et al.* 2019; Lindemann *et al.* 2020; Schaffer *et al.* 2020). However, not much is known about the history of the ice sheet of NE Greenland and its general sensitivity to atmospheric and ocean warming. Even to this day it remains a controversy among scientists if the ice sheet reached the shelf edge or not during the Last Glacial Maximum (LGM, 24–18 ka;

Lisiecki & Raymo 2005). The timing and pattern of ice retreat in NE Greenland during the deglaciation c. 18–10 ka are not well known, either.

The Fram Strait is today the only deep-water connection between the North Atlantic and Arctic Oceans and forms a major conduit for exchange of warm Atlantic Water and cold Polar Water. The East Greenland Current (EGC) flows southwards along East Greenland to the Denmark Strait and part of this water-mass enters the Atlantic Ocean. It carries cold, low-saline Polar Surface Water with sea ice and icebergs coming via the Trans-Polar Drift in the Arctic Ocean. The Polar Water overlays Atlantic Intermediate Water (AIW, i.e. Return Atlantic Water (RAW) and Arctic Atlantic Water (AAW)) and Arctic Ocean and Greenland Sea deep waters (e.g. Swift 1986; Aagaard & Carmack 1989; Hopkins 1991; Rudels *et al.* 2002, 2005; see details below; Fig. 1A, D). The variability of the EGC and sea ice cover on the NE Greenland shelf has been investigated for the Holocene interglacial (Notholt 1998; Syring *et al.* 2020a, b; Davies *et al.* 2022; Pados-Dibattista *et al.* 2022). So far, no

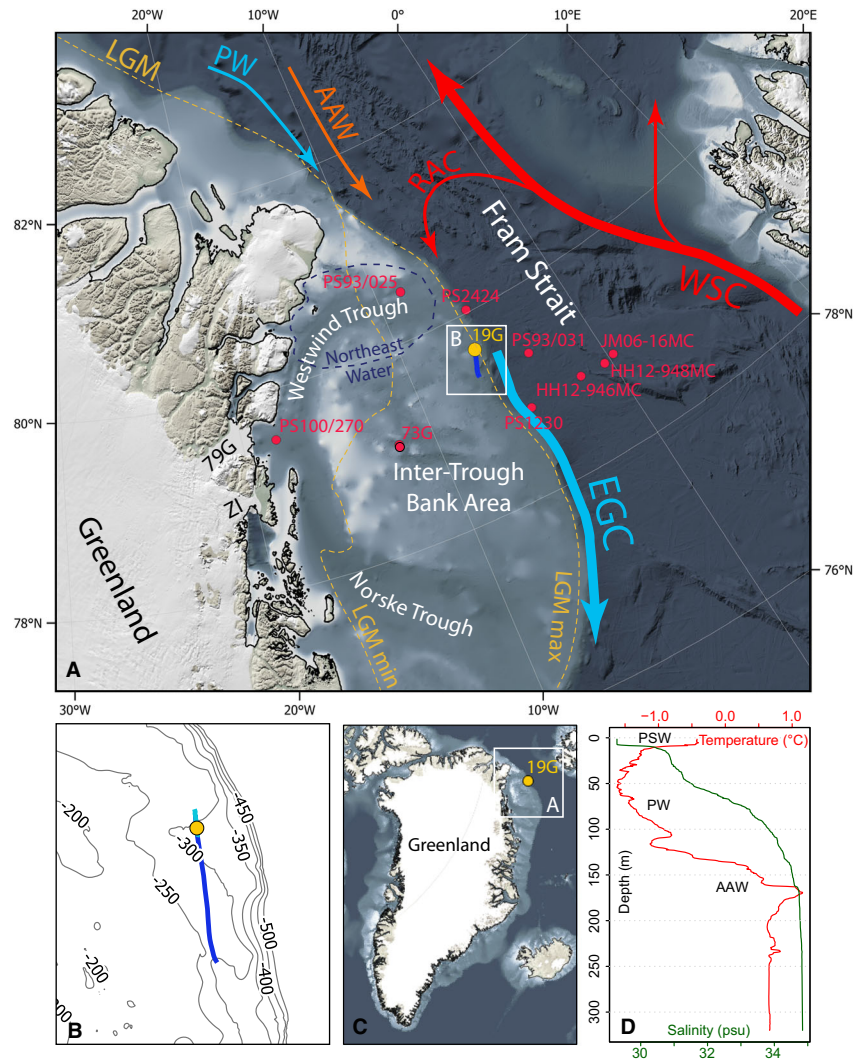


**Fig. 1.** A. Map of northern Nordic Seas (see overview map in C) with location of core DA17-NG-ST01-019G (19G) and major currents indicated; blue arrow = East Greenland Current (EGC); red arrow = West Spitsbergen Current (WSC). RAC = Return Atlantic Current; AAW = Arctic Atlantic Water; PW = Polar Water; ZI = Zachariae Isstrøm; 79G = Nioghalvfjærdsfjorden Glacier. Bathymetry from IBCAO v4 (Jakobsson *et al.* 2020) and position of the Northeast Water polynya from Sørensen (2012). Yellow stippled lines mark minimum (based on Funder *et al.* 2011 and Gowan *et al.* 2021) and maximum (based on Evans *et al.* 2009) limits of the NE Greenland Ice Sheet. Core records discussed in the text are marked in red. B. Detail of outer NE Greenland shelf area with sub-bottom profiler lines and location of core 19G marked. Bathymetry (m) from Arndt *et al.* (2017). Dark blue line shows location of seismic profile shown in Fig. 2A, and light blue line, the seismic profile shown in Fig. 2B. D. CTD (conductivity, temperature, depth) data from the core site with main water-masses indicated. PSW = Polar Surface Water.

core studies have targeted the palaeoceanographic conditions over the NE Greenland shelf during the last glacial period and the early deglaciation and the timing in relation to ice-sheet dynamics.

The NE Greenland shelf with its extensive, near-permanent sea ice cover has proven difficult to access for detailed geological surveys and sediment sampling. Patchy acoustic and shallow seismic surveys have been conducted in recent years (Evans *et al.* 2009; Arndt *et al.* 2017; Laberg *et al.* 2017; Olsen *et al.* 2020) with a more comprehensive bathymetry published by Arndt *et al.* (2015). The results of these studies have been interpreted to indicate that the NE Greenland Ice Sheet reached to the shelf edge across most or all of the region

(Fig. 1A). However, although these investigations have shown clear glacial landforms across the shelf, they do not offer any certain information of their age. Terrestrial and coastal studies have indicated that the ice sheet only reached onto the inner parts of the shelf during the LGM (e.g. Funder *et al.* 2011 and references therein), while some marine studies have indicated that the ice sheet may have reached to the mid-shelf (Evans *et al.* 2002; Winkelmann *et al.* 2010) (see also reviews by Vasskog *et al.* 2015 and Arndt *et al.* 2017). Studies on depositional patterns on the NE Greenland slope (72–75°N) have also suggested that ice streams did not reach the shelf edge during the late Weichselian (Wilken & Mienert 2006).

Here, we report results from a sediment core taken on the NE Greenland shelf edge at 79.4°N (Fig. 1A–C). The purpose of this investigation is to reconstruct the environmental development and past flow of the Polar and Atlantic Water over the shelf and to determine if the ice sheet reached our core site during the LGM. The study is based on detailed AMS-<sup>14</sup>C dating, distribution patterns of planktic and benthic foraminiferal assemblages, together with sedimentological, geochemical (XRF core scanning) and geophysical data, combining sediment core data with shallow seismic survey data from the area.

## Study area

The Fram Strait is bordered to the west by the NE Greenland shelf with an average water depth of ~300 m. It spans ~300 km at its widest point at ~77°N (Fig. 1A, C). It is of rugged topography with several shallow banks (part of the Inter-Trough Bank Area; Fig. 1A) surrounded by deep cross-shelf troughs from former ice streams (Westwind Trough and Norske Trough) (e.g. Jakobsson *et al.* 2012; Arndt *et al.* 2015). The troughs are ~310 and 325 m deep at the shelf edge, respectively, and each deepens westward towards land to >500 m water depth (Arndt *et al.* 2015). Morphologically, the shelf is characterized by numerous features witnessing the past activity of an ice sheet such as grounding zone wedges, retreat moraines, subglacial lineations, and numerous iceberg ploughmarks: the latter especially at the mid- and outer shelf (e.g. Evans *et al.* 2009; Winkelmann *et al.* 2010; Arndt *et al.* 2015).

The NE Greenland shelf area is covered by sea ice for most of the year. The shelf is also affected by icebergs coming from the Arctic Ocean, or derived from several large, fast flowing marine-terminating ice streams, namely Nioghalvfjærdsfjorden Glacier, Zachariae Isstrøm, and Storstrømmen (Fig. 1A). These ice streams together drain about 16% of the Greenland inland ice (Rignot & Mouginot 2012; Mouginot *et al.* 2015). Numerous polynyas are present in the inner part of the shelf, where the Northeast Water Polynya is the most stable and the most studied example (e.g. Newton & Rowe 1995; Kohfeld *et al.* 1996; Syring *et al.* 2020a, b; Fig. 1A). In the polynya with seasonal open water conditions, productivity is high for a polar environment, and thus can support a richer foraminiferal fauna than in areas under permanent sea ice cover (Newton & Rowe 1995).

In the eastern Fram Strait, the West Spitsbergen Current (WSC) carries warm Atlantic surface water along the Svalbard Archipelago and into the Arctic Ocean (Fig. 1A). In the western Fram Strait over the NE Greenland shelf, the southward flowing EGC brings cold Polar Surface Water, and warmer subsurface AIW (e.g. Rudels *et al.* 2002, 2005; De Steur *et al.* 2009; Zamani *et al.* 2019; Fig. 1A). The bottom water of the banks of the inner NE Greenland shelf is primarily influenced by

the relatively cold Arctic Atlantic Water (AAW), which is derived from the AIW after it has circulated the Arctic Ocean at subsurface levels (e.g. Rudels *et al.* 2002, 2005; De Steur *et al.* 2009; Zamani *et al.* 2019; Fig. 1A). The bottom water of the outer part of the shelf south of 79°N is influenced by the warmer subsurface Return Atlantic Water (RAW; Rudels *et al.* 2005; De Steur *et al.* 2009). The RAW is transported by the Return Atlantic Current (RAC), which diverges from the WSC towards the East Greenland slope and shelf before flowing south towards the Denmark Strait (Fig. 1A). The warm RAW also reaches the inner shelf through the deep troughs crossing the shelf, causing increased melting rate of the marine-terminating glaciers, inclusive the Nioghalvfjærdsfjorden Glacier (Lindemann *et al.* 2020; Schaffer *et al.* 2020). The RAW forms the warmest part of the Atlantic Water of the EGC, while the AAW entering from the Arctic Ocean is considerably colder (e.g. Rudels *et al.* 2002, 2005). Differences in temperature and salinity cause the water column to be strongly stratified between the upper Polar, cold layer and the warmer and saltier AAW/RAW underneath.

Our core site is located in a southeast facing inlet on the northeastern outer part of the Inter-Trough Bank Area close to the mouth of the Westwind Trough (Fig. 1A, B). The inlet opens towards the slope, forming a minor shelf-edge inlet (Fig. 1B). The water depth at the mouth of the inlet is 330 m, i.e. similar to the water depth in the outer Westwind Trough.

## Material and methods

### CTD profile

A conductivity-temperature-depth profile (CTD; DA17-NG-ST01-001CTD) was measured down to 320.9-m depth along a vertical depth profile at latitude 79°37.236'N, longitude 006°03.535'W using the SEA-BIRD 911 system of RV 'Dana', to identify the different water-masses.

### Sediment core handling and data

Gravity core DA17-NG-ST01-019G (hereafter core 19G) was taken at 322.5-m water depth inside the shelf-edge inlet at 79°38.027'N, 006°03.070'W on 13th September 2017 during a cruise with RV 'Dana' to the NE Greenland shelf (NorthGreen2017 Expedition; Seidenkrantz *et al.* 2018; Fig. 1A, B).

Onboard, the 1.51-m-long gravity core was divided into ~0.5 and 1 m sections and stored at ~3 °C. After return to the laboratory at Aarhus University, the core sections were split lengthwise, and the sediment described. The archive halves of the core were scanned with an Itrax X-ray fluorescence (XRF) core scanner (Cox Analytical) at the Department of Geoscience, Aarhus University, Denmark. The scan was performed

with a molybdenum tube at a step size of 200  $\mu\text{m}$ , with a 10-s exposure time (voltage: 30 kV, current: 40 mA). The core scanning provided a line scan image, which is a 2-cm-wide radiographic image of the centre of the core (voltage: 60 kV; current: 50 mA; exposure time: 2000 ms). The obtained radiographic image was digitally enhanced by processing the raw data files using the algorithm presented by Löwemark *et al.* (2019). The colour of the radiographic image is a measure of sediment density. From the results of the scanning of the bulk geochemical composition, we show the element counts of Fe (in counts per second, cps) and the ratio of Ca/Fe. This ratio reflects the content of mainly biogenic  $\text{CaCO}_3$  compared to Fe that reflects the detrital, terrigenous component of the sediment supply (Richter *et al.* 2006; Rothwell & Croudace 2015). The magnetic susceptibility was measured every 0.5 cm using a Bartington magnetic susceptibility system, with a MS2E high-resolution point-sensor and a MS2I Sensor, mounted within the ITRAX core scanner.

The working halves of the gravity core were sampled in 1-cm-thick slices at 4-cm intervals for foraminiferal and grain-size analysis. The wet samples were weighed and directly sieved over sieves with mesh-sizes 0.063, 0.100 and 1 mm. The sample residues were dried and weighed, and weight percent of each size fraction calculated vs. the sample wet weight. The size fraction >1 mm was counted for ice-rafted debris (IRD) and concentration (number per gram wet weight sediment) was calculated. Planktic and benthic foraminifera were counted in the 0.1–1 mm size fraction (>250–>300 specimens of each) and number of specimens per gram wet sediment was calculated. Most samples were very rich in foraminifera >0.1 mm. The size-fractions 0.063–0.1 mm were checked for foraminiferal content; the lower part 151–60 cm down core was practically barren of foraminifera. In the interval 50–30 cm, a low number of the same species as occurring in the size-fraction 0.1–1 mm were found, while in the upper 30 cm, a few agglutinated specimens occurred. We are therefore confident that results from the counts of the 0.1–1 mm size fraction are reliable.

Benthic and planktic foraminifera were identified to species level in most cases. Species of small *Elphidium* and *Buccella* were only identified to genus level and miliolid species were grouped as ‘miliolids’. Relative abundances of planktic foraminiferal species were calculated based on the planktic assemblage alone, while those for the benthic foraminifera were calculated

based on the total benthic calcareous and agglutinated assemblages. A complete list of encountered species is found in Table S1.

The lower part of the core contained numerous well-preserved foraminifera, while samples in the upper 30 cm were very low in foraminifera and consisted mainly of agglutinated species and no planktic foraminifera. In two samples (24.5 and 28.5 cm), only 16 and 82 benthic specimens, respectively, could be obtained in total.

Planktic/benthic ratios were calculated by dividing concentrations of planktic by concentrations of benthic specimens. For planktic foraminifera, small shell fragments of specimens were counted on a semi-quantitative basis (only a few squares on the picking tray were counted) and concentration calculated. Percent fragmentation was calculated as number of fragments relative to the concentration of whole planktic specimens plus fragments. All percentage data of the most common species, and absolute abundances can be found in Table S2.

Accelerator mass spectrometry (AMS)  $^{14}\text{C}$  dating was performed on mixed benthic (excluding miliolids) and planktic foraminiferal faunas or macrofossils (encrusting bryozoans and a fragmented bivalve *Portlandia arctica*) at the dating facility at the Department of Physics and Astronomy, Aarhus University, Aarhus, Denmark (Table 1). The  $^{14}\text{C}$  dates were calibrated to calendar ages before the year 1950 using the Calib7.04, Marine13 program adding a  $\Delta R$  value for NE Greenland of 150 years (Reimer *et al.* 2013; Table 1).

#### Geophysical data

The geophysical data comprise sub-bottom profiles acquired with a parametric Innomar SES-2000 Deep instrument hull-mounted on RV ‘Dana’. A low frequency (LF) ping signal of 6 kHz, emitted with four pulses at a time, and a recording length of 30–50 m was used. Post-cruise processing of the data included corrections of navigation issues, application of a swell filter to reduce some of the effects from heave variations, and some smoothing of the data by stacking. Data interpretation was done using the IHS Markit Kingdom seismic interpretation software and included identification of seabed morphologies such as iceberg ploughmarks and mapping of sediment basins and some deeper structures (Fig. 2). A sediment velocity of 1600  $\text{m s}^{-1}$  and a water

Table 1. Radiocarbon dates and calibrated ages for core DA17-NG-ST01-019G.

Depth (cm)	AMS $^{14}\text{C}$ age (a BP; 1 $\sigma$ error)	Cal. age(a BP; 1 $\sigma$ error)	Lab. code	$\delta^{13}\text{C}$ AMS	Material
32.5	8721 $\pm$ 38	9210 $\pm$ 69	AAR-30033	3 $\pm$ 1	Mixed P. and B. foram.
72.5	16 717 $\pm$ 91	19 499 $\pm$ 133	AAR-30036	0 $\pm$ 1	Bryozoan
92.5	18 287 $\pm$ 109	21 470 $\pm$ 182	AAR-30035	-1 $\pm$ 1	Bryozoan
124.5	14 929 $\pm$ 69	17 520 $\pm$ 108	AAR-30034	0 $\pm$ 1	<i>Portlandia arctica</i> fragment
150.5	21 714 $\pm$ 119	25 520 $\pm$ 138	AAR-29384	3 $\pm$ 1	Mixed P. and B. foram.

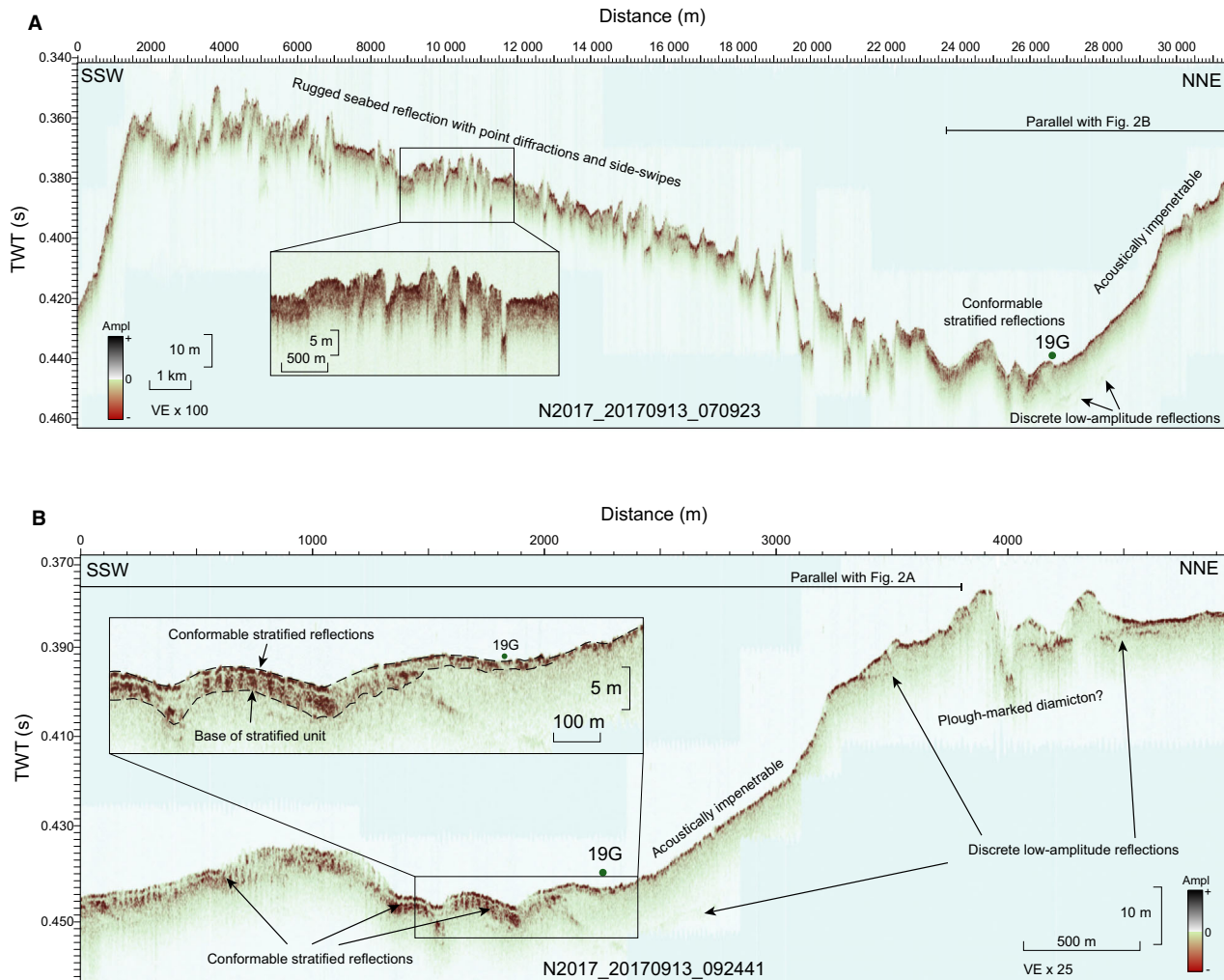


Fig. 2. Sub-bottom profiler data showing the 19G core site in relation to the bathymetry and seabed morphology. South and west of the core site, note rugged seabed with numerous incisions indicative of iceberg scouring (A = dark blue line in Fig. 1B). Close to the core site, the seabed is underlain by a unit with stratified reflectors of 1–3 m thickness, decreasing in thickness towards the core site 19G (B = light blue line in Fig. 1B). TWT = two-way-travel time. For depth conversion of the TWT, a sediment velocity of  $1600 \text{ m s}^{-1}$  and a water column velocity of  $1500 \text{ m s}^{-1}$  are used.

column velocity of  $1500 \text{ m s}^{-1}$  were used for depth conversion.

## Results

### CTD data

The CTD data acquired at the core location show presence of AAW at the bottom with temperature around  $0.66 \text{ }^\circ\text{C}$  and salinity of 34.84 psu (Fig. 1D; e.g. Rudels *et al.* 2005). Polar Surface Water with temperature of  $\sim -1.5 \text{ }^\circ\text{C}$  and salinity down to 31 psu occurs between  $\sim 20$  and 150 m water depth. At the surface a thin layer of low saline Polar Water with slightly higher temperature occurs ( $T = -0.5 \text{ }^\circ\text{C}$ ,  $S = 29.29$  psu) interpreted as a summer mixed layer of meltwater warmed by the sun.

### Lithology, grain sizes and foraminiferal content

Core 19G consists mainly of fine silty clay of light grey colour (Fig. 3, left column). The presence of a 1–2 cm thick oxidized layer at the core top and of a few diatoms and radiolarians in the top 0–1 cm sample indicates that most of the surface sediments are preserved. The lower part of the core (151–58 cm) consists of a diamicton of relatively coarse, unsorted sediments ( $>12$ – $15\%$  coarse clasts  $>1 \text{ mm}$  and  $10$ – $15\%$  between 0.1 and 1 mm by weight) in a relatively fine-grained matrix (Fig. 3E). The X-ray scan image shows variable density, especially in the lower part below 110 cm indicating that the deposit is not entirely uniform and massive (Fig. 3A; high-resolution images of the XRF core scan can be found in Fig. S1). The sediment contains abundant planktic and benthic foraminifera and numerous macrofossils,

including fragile sessile bryozoans (Fig. 4B, C). The content of IRD (no. IRD  $g^{-1}$  wet weight sediment) is relatively stable and consists mainly of quartz and some reddish feldspar-rich granite fragments. The concentrations of benthic and planktic foraminifera (no. B  $g^{-1}$  and P  $g^{-1}$  wet weight sediment, respectively), planktic/benthic (P/B) ratio, and percent planktic foraminiferal fragmentation show nearly constant values (Fig. 4). The interval ~46–30 cm shows a decrease in concentration of IRD and a varying, but high number of foraminifera, accompanied by a rise in % fragmentation. At ~40 cm, a marked change is seen in the X-ray scan indicating a change from high density sediments to low density sediments (Fig. 3A); however, most other parameters show no change at this point (Figs 3–5; see below). At 32 cm, a sharp peak in IRD is seen (Fig. 4A). Except for this IRD peak, the upper 40 cm consist mainly of fine clayey sediment without any coarse material (Fig. 3E).

The magnetic susceptibility record shows highest values in the lower part (151–58 cm), slightly lower values from 58 to ~25 cm, and lowest values in the upper ~25 cm (Fig. 3B). The Fe counts show a characteristic peak at 58–56 cm (Fig. 3C) above a clear and sharp lithological boundary as seen in the XRF-image (Figs 3, S1). The Ca/Fe ratio shows high values in the lower

151–58 cm interval, medium values in the 58–~30 cm interval, and very low values in the upper ~30 cm (Fig. 3D). Generally, the concentrations of foraminifera and macrofossils follow the Ca/Fe ratio, indicating highest content of  $CaCO_3$  in the lower, coarse part, medium in the foraminifera-rich part (but of high % fragmentation of planktic foraminifera), and lowest in the upper 24 cm, where mostly agglutinated foraminifera are preserved (Figs 3D, 4B, C, G).

#### Benthic and planktic foraminiferal species distributions

Three main planktic foraminiferal species were found: *Neogloboquadrina pachyderma*, *Turborotalita quinqueloba* and *Neogloboquadrina incompta*. *Turborotalita quinqueloba* only occurs in sediments below 58 cm. *Globigerinita glutinata* is rare with sporadic occurrences. The planktic fauna is entirely dominated by *N. pachyderma* (89–98%; Fig. 4F). There are no planktic foraminifera in the top 27 cm of the core.

The benthic foraminiferal faunas consisted of >42 calcareous species/species groups and >16 agglutinated species/species groups (exclusive of suspected reworked species; see Table S1). For the benthic foraminifera, we focus mainly on calcareous species with relative abundance above 5% in at least one sample, except for the

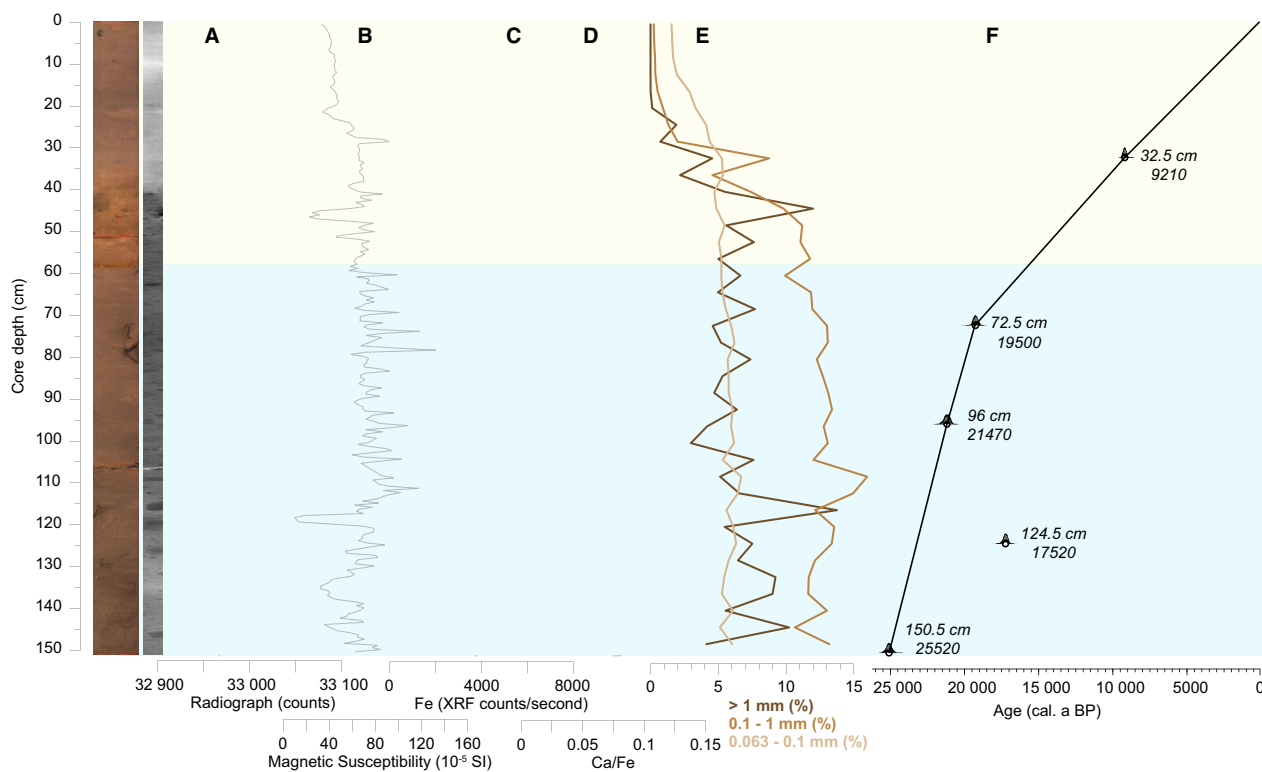


Fig. 3. Line scan and radiographic (X-ray) images of core 19G, lithological log, and measurements from the ITRAX core scanner. A. Radiograph (a measure of density; note dark colours correspond to high density, light colours to low density). B. Magnetic susceptibility. C. Fe (counts per second (cps)). D. Ca/Fe ratio. E. Grain size in % grains >1, 0.1–1 and 0.063–0.1 mm calculated vs. total sample weight. F. Age-depth plot and age model of core 19G with calibrated (cal.) AMS- $^{14}C$  ages indicated (see also Table 1). A high-resolution figure of line scan and radiographic X-ray images is shown in Fig. S1.

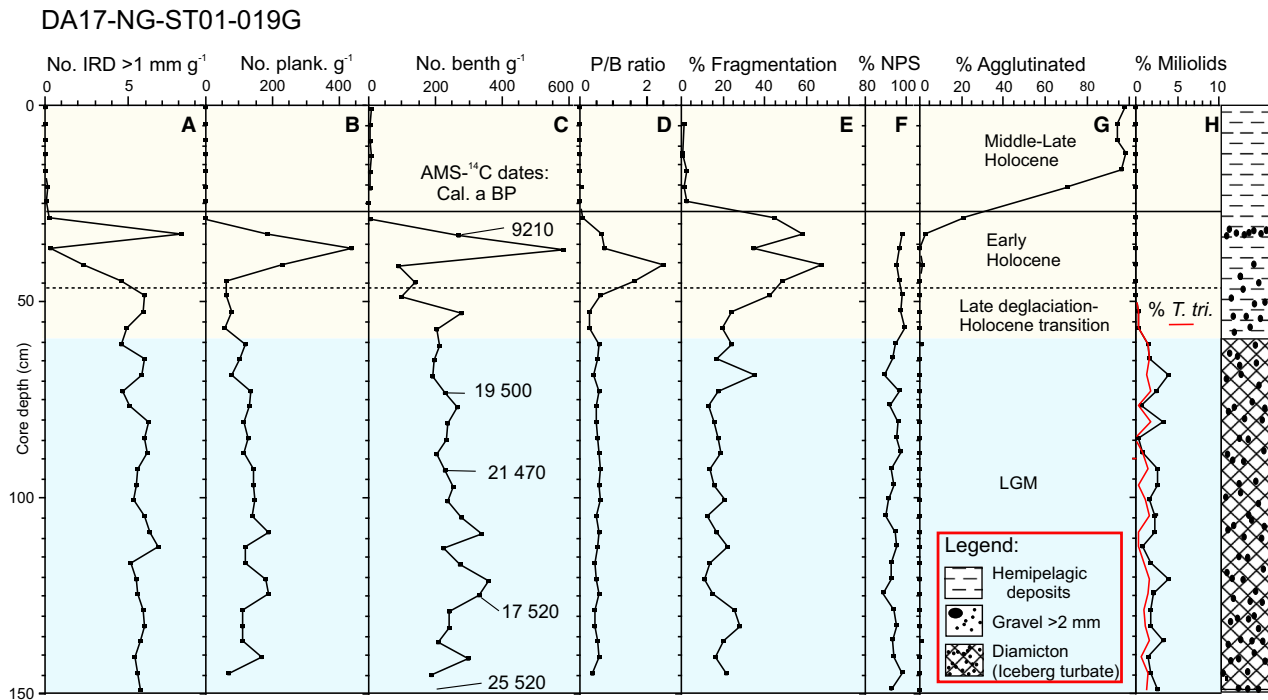


Fig. 4. A. Concentration of ice-rafted debris (IRD) in the size fraction  $>1$  mm (no. mineral grains per gram wet weight (wwt) sediment). B. Concentration of planktic foraminifera (no. of specimens per gram wwt sediment). C. Concentration of benthic foraminifera (no. of specimens per gram wwt sediment) with calibrated (cal.) AMS- $^{14}\text{C}$  ages shown. D. Planktic/benthic (P/B) ratio. E. % fragmentation (see text for explanation). F. % *Neogloboquadrina pachyderma* s (NPS). G. % Agglutinated benthic foraminiferal specimens. H. % Miliolida (all miliolid species added together, inclusive of *Triloculina trihedra* (shown by red curve)). Column to the right shows lithological log. Stratigraphical intervals and legend are shown in panel G: LGM = Last Glacial Maximum (24–17.5 ka); Late deglaciation to Holocene transition ( $>11.7$  ka); Early Holocene (11.7–7.5 ka); Middle–Late Holocene (7.5–0 ka).

miliolid species *Triloculina trihedra* that despite never exceeding 2% is persistent in the glacial samples (Fig. 4H).

The benthic fauna is dominated by *Cassidulina reniforme*, *Cassidulina neoteretis* and *Cibicides lobatulus*, followed by *Elphidium clavatum*, *Elphidium hallandense*, *Buccella* spp. and *Islandiella* spp. (predominantly *I. norcrossi*) as accessory species. *Trifarina fluens* is present in one sample at close to 10% but is otherwise very rare (Fig. 5J). *Melonis barleeanus* and *Astrononion gallowayi* are both present below 27 cm, but rarely exceed 5%, while miliolid species (predominantly *T. trihedra*) and *Glabratella arctica* are only found below 58 cm not exceeding 4 and 3%, respectively (Fig. 5; Table S2). *Nonionellina labradorica* and *Stainforthia loeblichii* show a consistent presence, not exceeding 2%. *Pullenia bulboides* and *Alabaminella weddellensis* (the latter also called *Epistominella nipponica* in the Barents Sea; Hald & Steinsund 1992) are rare and only present in a few samples (Table S2).

Above 27 cm, most calcareous species decline rapidly and disappear, and the benthic foraminiferal fauna consists almost entirely of agglutinated species of low concentration (Figs 3G, 4). This fauna is dominated by *Ammoglobigerina globigeriniformis*, *Portatrochammina bipolaris*, *Lagenammina difflugiformis*, *Reophax scori-*

*urus* and *Adercotryma glomerata*. *Deuterammina montagui* reaches up to 7% and *Reophax fusiformis* to almost 6%, otherwise most other species (*Recurvoides turbinatus*, *Spiroplectammina biformis*, *Cribrostomoides crassimargo* and *Textularis torquata*) rarely exceed 3% (Table S2).

#### Observations and interpretations from sub-bottom profiler data

The sub-bottom profiler data passing over the 19G position show that the core site is situated inside the small shelf-edge inlet on the northeastern part of the Inter-Trough Bank Area south of the mouth of the Westwind Trough (Figs 1B, 2). Overall, the profiler data show a generally rugged seabed morphology underlain by a transparent/homogenous succession with a few discrete low-amplitude internal reflectors (Fig. 2B). Within the inlet, the seabed reflector is coherent with a hummocky morphology and underlain by a conformable stratified succession up to 3 m thick that thins towards the 19G core site to  $<1$  m thickness (Fig. 2B). The seabed reflector south- and westwards of 19G is irregular and rugged with incisions of varying size, typically 50–300 m wide and 2–12 m deep, with the largest reaching up to 600 m in width and 23 m in depth (Fig. 2A). The

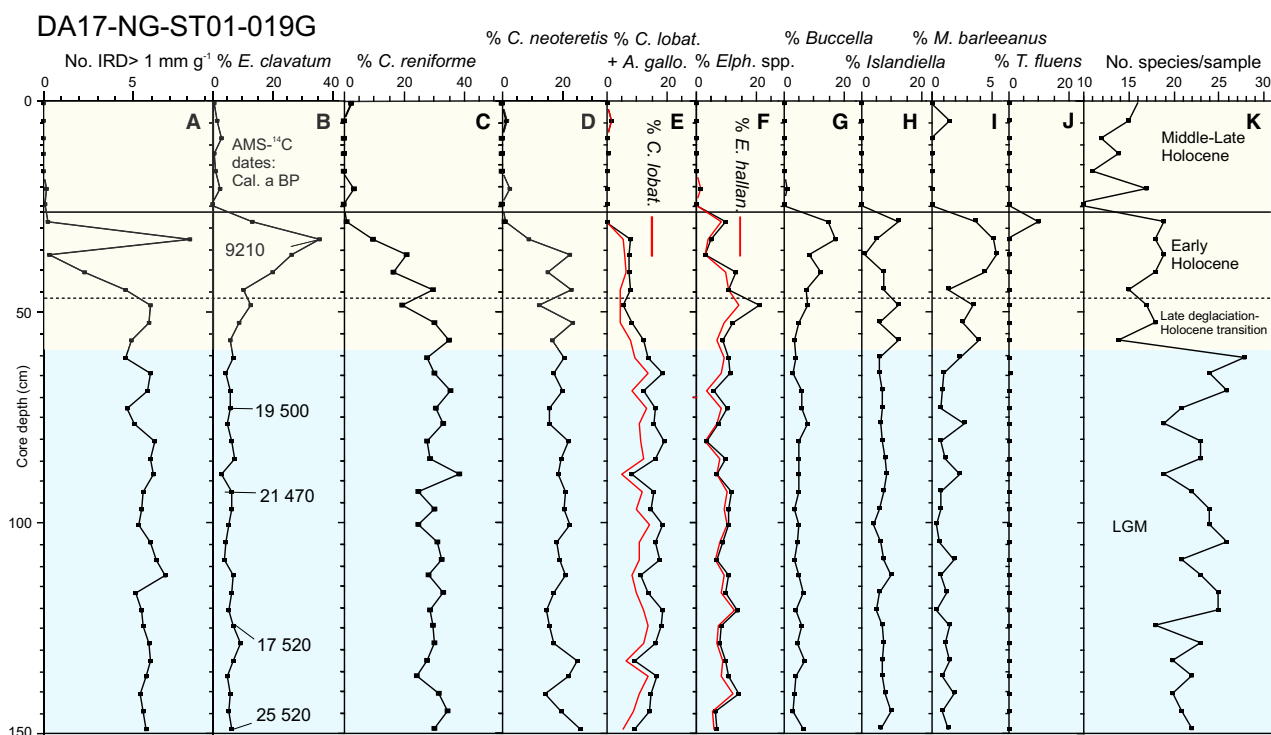


Fig. 5. A. Concentration of IRD from Fig. 4. B. % *Elphidium clavatum* with calibrated (cal.) AMS-<sup>14</sup>C ages shown. C. % *Cassidulina reniforme*. D. % *Cassidulina neoteretis*. E. Cumulative plot of % *Cibicides lobatulus* and *Astrononion allowayi*. F. Cumulative plot of % *Elphidium hallandense* and *Elphidium* spp. G. % *Buccella* spp., H. % *Islandiella* spp. (predominantly *I. norcrossi*). I. % *Melonis barleeanus*. J. *Trifarina fluens*. K. Diversity of benthic species as number of species in a sample and with stratigraphical intervals indicated: LGM = Last Glacial Maximum (24–17.5 ka); Late deglaciation to Holocene transition (>11.7 ka); Early Holocene (11.7–7.5 ka); Middle–Late Holocene (7.5–0 ka).

ruggedness is associated with many point diffraction hyperbolae and sideswipe reflections (Fig. 2A). The flank of the inlet northward of the 19G site is characterized by a relatively smooth, southeastward dipping slope (~2.5°). On top of the slope, where water depth has decreased to ~290 m, there is a ~1.4 km long and up to 10 m high, transparent unit with large, up to 15 m deep incisions (Fig. 2B).

The rugged and heavily incised seabed reflector indicates a morphology comprising lineaments or gutters in a crisscrossed pattern. We interpret this as the result of dense iceberg ploughing on the outer Inter-Trough Bank Area (Figs 1A, 2) in accordance with observations by Arndt *et al.* (2017). The occurrence of conformable stratified reflections in the area where the gravity core was retrieved suggests that sediments were trapped in the inlet. The large incisions and transparent character of the unit observed north of the inlet resemble an iceberg-ploughed diamicton, the origin of which cannot be determined based on the limited present data set.

## Discussion

### Chronology

Based on the above clear changes in lithology, magnetic susceptibility, foraminiferal faunas and the trend in the

Ca/Fe ratio, we divide the record into three sections: 151–58, 58–27 and 27–0 cm (Figs 3–5). The subdivision into three horizons matches the sub-bottom profiler data at the core site, which show a relatively thin <1-m stratified succession at the top and a transparent/homogenous interval at the base (Fig. 2B).

The lower part dates from *c.* 25.5 cal. ka at the core bottom (150.5 cm) to 19.5 cal. ka (72.5 cm). One age reversal is observed with a younger age of 17.5 cal. ka at 124.5 cm (Table 1, Fig. 3F). Nevertheless, the dates on the macrofossils indicate an LGM and early deglaciation age of the coarse-grained deposit below ~58 cm in the record.

In the interval 58–36 cm there are no dates available, mainly due to poor preservation and absence of suitable macrofossils and foraminifera. A gradual change in most parameters is seen (Figs 3–5). The date of 9210 cal. years at 32.5 cm indicates that most of the upper part of core 19G is of Holocene age (Figs 3–5, Table 1). At ~46 to ~27 cm, the % fragmentation is at its maximum and concentration of benthic and planktic foraminifera peaks (Fig. 4B, C, E). Given the maxima in foraminiferal concentrations and the small peaks in % *C. neoteretis*, *C. reniforme*, *M. barleeanus* and *P. bulloides* (Figs 4B, C, 5C, D; Table S2), this interval is interpreted to comprise the Early Holocene (see interpretations of the foraminiferal species distribution below). We have ten-

tatively marked the start of the Holocene at 46 cm where % fragmentation and the P/B ratio increase and many species change in relative abundance (stippled line in Figs 4, 5). The change in sediment density seen in the X-ray scan at 40 cm probably marks the transition from glaciomarine sedimentation to hemipelagic sedimentation (Figs 3, S1). The sharp peak in IRD at 9210 cal. years probably represents the final deglaciation (Fig. 4A). Similar abrupt peaks in ice-rafting have been observed at the western and northern Svalbard margins in the eastern Fram Strait – here dating to *c.* 10 cal. ka (Ślubowska-Woldengen *et al.* 2007).

Assuming linear sedimentation rates, and that the core top has preserved near-recent sediments, the interval 27–0 cm with no dates and only agglutinated foraminifera is here tentatively referred to the period from *c.* 7.5–*c.* 0 ka, i.e. Middle–Late Holocene to Recent (Figs 3, 4).

#### Interpretation of palaeoceanography and sedimentary environments

*Lower section 151–58 cm (LGM and early deglaciation 25–*c.* 17.5 ka): extensive Atlantic Water inflow and iceberg ploughing.* – The presence of rich planktic and benthic micro- and macrofaunas is a clear indication that the core site was not overrun by an ice sheet during the LGM (Figs 4, 5). The planktic foraminiferal fauna is dominated by *N. pachyderma* and *T. quinqueloba* in high abundances; this assemblage is typical of modern Polar environments in the Arctic Ocean and the central and western Fram Strait (e.g. Kohfeld *et al.* 1996; Carstens *et al.* 1997; Pados & Spielhagen 2014; Fig. 4F, Table S2). The benthic foraminiferal fauna consists of an assemblage of marine species typical for Arctic and Polar shelf areas, with many species linked to Polar Water, others primarily to Atlantic-sourced water (RAW or AAW) (Fig. 5; see discussion below). The foraminifera are well preserved (low % fragmentation) and co-occur with numerous molluscs (gastropods including pteropods, bivalves, scaphopods), branched and encrusting bryozoans, calcareous polychaete tubes (genus *Spirorbis*) still attached to rocks and bryozoans, and remains of ophiurians (brittle-stars) (Figs 4E, 6, S2). As the pteropods and bryozoans are very fragile, reworking by an ice sheet is unlikely (Fig. 2A, B). Combined with the abundant presence of IRD in an otherwise fine-grained matrix (diamicton deposit), we interpret that the sediment was deposited in a glaciomarine environment.

*Cassidulina reniforme* and *C. neoteretis* are the dominant species followed by *C. lobatulus* (Fig. 5C, D, E, Table S2). *Cassidulina neoteretis* is associated with Atlantic Water of relatively high BWT, often under stratified conditions with perennial or near-perennial sea ice cover (Jennings & Helgadottir 1994; Seidenkrantz 1995; Lubinski *et al.* 2001; Cage *et al.* 2021). High relative abundance of *C. neoteretis* is

generally taken as evidence for an increased influence of Atlantic-sourced water (Jennings & Weiner 1996). Although *C. reniforme* is characterized as an Arctic glacier-proximal species, mapping of the species in the Barents Sea has revealed a dual distribution pattern; it is abundant close to glaciers in Polar Waters, but also found in high numbers in sandy, current influenced areas on and along banks together with *C. lobatulus*, and is here associated with the presence of chilled Atlantic Water and bottom currents (Hald & Steinsund 1992; Steinsund 1994; Korsun & Hald 2000). Thus, the presence of *C. neoteretis* and *C. reniforme* indicates relatively warm and saline bottom water temperatures likely reaching temperatures warmer than today. This may indicate that RAW at times was found at higher latitudes during the LGM than today, where AAW (0.66 °C) is present (Fig. 1D). The relatively high percentages of *C. lobatulus* and *A. gallowayi* (Fig. 5E) also suggest strong bottom current activity (cf. Wollenburg & Mackensen 1998). Furthermore, the low relative abundance of the polar species *E. clavatum* (a species typically associated with ice-proximal conditions, low BWT, low salinity, and high turbidity (Hald & Korsun 1997; Korsun & Hald 2000)) points to ice-distal conditions (Fig. 5B). The diversity (number of species in a sample) and concentrations of foraminiferal specimens are also fairly high for this northern latitude (Figs 4B, C, 5K). Encrusting and branched bryozoans are frequent today on the NE Greenland shelf, attached to dropstones that provide a hard bottom in otherwise soft sediments (Kuklinski & Bader 2007). As sessile organisms, they are dependent on strong bottom currents to bring food and oxygen indicating similar conditions during the LGM as today (Fig. 6). Together with the benthic foraminiferal faunas, the environment is thus interpreted as mainly influenced by warmer Atlantic-sourced water of strong currents bringing food below an extensive sea-ice covered and stratified upper water column. The relatively high concentration of coarse mineral grains (IRD >1 mm) indicates presence of icebergs (Fig. 4A).

To our knowledge, few high Arctic shelf records from the LGM containing abundant foraminifera exist. Two records from the shelf of southern Svalbard (76°N) at 389-m water depth contained sediments dating from the late glacial maximum 20–18.8 ka (Rasmussen *et al.* 2007; El bani Altuna *et al.* 2021a). These records show dominance of *C. neoteretis* together with *C. reniforme*, *E. clavatum* and some *C. lobatulus* and *M. barleeanus*, and bottom water temperatures reconstructed from Mg/Ca reach 4.4 °C. Notholt (1998) dated a core PS2424-1 (Fig. 1A) from NE Greenland from the very upper slope at 445-m water depth at ~80°N. This core spans the time interval 21 155–8190 years comprising the mid-late LGM into the Early Holocene. The sediments from the LGM are rich in planktic and benthic foraminifera (*N. pachyderma*, *C. lobatulus*, *C. neoteretis*, *Buccella*) and very similar to the fauna

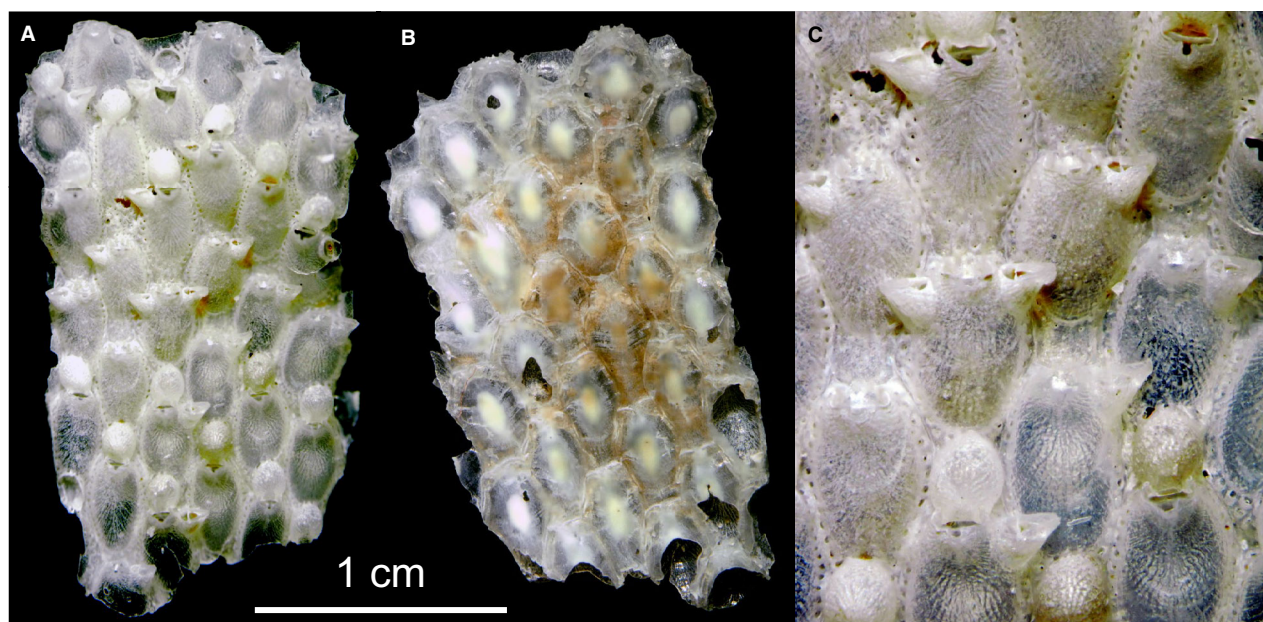


Fig. 6. Bryozoan specimen from 100.5 cm down-core. A. Front view. B. Back view. C. Close-up of chambers, front view. Although unidentified, it is of the same species as the AMS- $^{14}\text{C}$  dated specimens from 72.5 and 92.5 cm in core 19G (see Table 1).

in the LGM sequence in core 19G (Figs 4F, 5D, E, G). Further afield, two sedimentary records from the northern Labrador Sea and Davis Strait, respectively, also suggest a stronger-than-present influx of warm Atlantic-sourced water at both intermediate and deep-water levels under near-perennial sea ice cover (Seidenkrantz *et al.* 2019, 2021).

In core 19G, the records of the LGM section are all suspiciously constant giving almost straight curves (Figs 3–5). The covered time interval, the LGM and early deglaciation normally shows great variability in all of these parameters due to a high degree of environmental instability (e.g. Johnsen *et al.* 1992; Nam *et al.* 1995; Weinelt *et al.* 2003; Müller & Stein 2014; El bani Altuna *et al.* 2021b). This smoothing of signals in the 19G records could indicate some extent of ‘homogenization’ of the sediment and the foraminifera – i.e. that the deposits are partly mixed. The AMS- $^{14}\text{C}$  dates are mostly in chronological order with one exception (Fig. 3F, Table 1). A fragmented bivalve gave the reversed date, and the specimen could potentially have been mixed into older sediments during the coring process, but as we selected specimens not directly at the rim of the core, down-core transport of the shell is less likely. An alternative cause of the age reversal may be that the shell was transported downwards during mixing of the sub-sea floor sediment sometime after deposition (but prior to coring). The sub-bottom profiler data indicate some topography around the core site with a  $2.5^\circ$  slope towards the north (Fig. 2B). Such topography may have facilitated down-slope sediment processes locally, but since the slope surface above the core site shows no evidence of

slide scars, slope failure is considered unlikely (Fig. 2B). Winnowing by bottom currents could also create a smoothed record but is contradicted by the relatively coarse and unsorted sediments (Fig. 3). Reworking by an ice sheet is also unlikely due to the presence of the numerous, well-preserved macrofaunas including bryozoans (Fig. 6) and with *Spirorbis* worms still attached to bryozoans and gravel (Fig. S2). Instead, mixing of sediments by iceberg ploughing has been shown to leave relatively undisturbed sedimentary records in the sense that foraminifera and macrofaunas get mixed, but they remain both numerous and well preserved (Vorren *et al.* 1983; Hald *et al.* 1990). We thus interpret the lower section most probably to be an iceberg turbate cf. Vorren *et al.* (1983), where icebergs have ploughed and partly mixed the marine sea-floor sediments. A similar scenario can be observed in the sub-bottom profiler data (Fig. 2) where the rugged seabed, the many diffractions and the sideswipe reflections are interpreted to be formed due to iceberg ploughing.

*Mid-section 58–27 cm (late deglacial transition and Early Holocene c. 11–c. 7.5 ka): gradually diminishing Atlantic Water inflow.* – The lower part of the mid-section consists of a thin horizon (58–46 cm) showing a sharp boundary to the underlying coarse unsorted glaciomarine diamicton marked by the high peak in Fe counts at 58–56 cm (Fig. 3). The interval 58–46 cm otherwise shows a gradual transition in most parameters along with a gradual decline in concentration of IRD (Figs 4, 5). Most likely, this indicates cessation of iceberg ploughing and that the interval may belong to the late

deglacial transition to the Early Holocene, but without dates this is uncertain. The most distinct change is the abrupt decrease in diversity of the benthic foraminifera and the sudden drop in the Ca/Fe ratio at 58 cm, while *E. clavatum* increases gradually, along a decline of the current-indicator species *C. lobatulus*, and *A. gallowayi* (Figs 3D, 5B, E). The decrease in the Ca/Fe ratio may reflect an increase in supply of terrigenous material compared to biogenic CaCO<sub>3</sub> (Fig. 3D).

At ~46–27 cm (Early–Middle Holocene), the % fragmentation is at a maximum (60%), indicating poor preservation (Fig. 4E). *Cassidulina reniforme* and *C. neoteretis* first peak in relative abundance and subsequently decline (Fig. 5C, D). This indicates that the inflow of Atlantic-sourced water remained high in the Early Holocene, but also that it was diminishing with time (see below). During the Early Holocene on the inner NE Greenland shelf (core PS100/270; Fig. 1A), *C. neoteretis* and *C. reniforme* likewise dominate with up to >80 and 60%, respectively, together with maximum flux of both benthic and planktic foraminifera (Syring *et al.* 2020a). Sea-ice proxy IP<sub>25</sub> and other biomarker data from core PS93/025–2 (Fig. 1A) indicate decreased, but variable sea ice cover on the mid-shelf (Syring *et al.* 2020b), with likely a higher degree of sea ice than on the outer shelf, where *C. neoteretis* and *C. reniforme* peak at 30 and 25%, respectively (Fig. 5C, D). Similar faunas as in core 19G are also found in many Early Holocene records from East Greenland shelf areas along the southeastern margin both south and north of the Denmark Strait (Jennings *et al.* 2002, 2011), central East Greenland off Scoresby Sund (Perner *et al.* 2015) and on the NE Greenland shelf in cores PS2424-1, PS100/270, and DA17-NG-ST07-073G (core 73G) (Fig. 1A) (Notholt 1998; Syring *et al.* 2020a; Pados-Dibattista *et al.* 2022, respectively).

*Elphidium clavatum*, *Elphidium* spp., *Buccella* spp., *Islandiella* spp., *M. barleeanus* and agglutinated specimens increase in the upper part of the Early Holocene interval (Figs 4G, 5B, F, G, H, I). They are all typical members of the modern Northeast Water Polynya assemblage located on the inner NE Greenland shelf where productivity is increased (Newton & Rowe 1995), thus indicating more open surface water conditions, reduced stratification, and higher seasonal food supply. The concentrations of benthic and planktic specimens reach a maximum, also pointing to increased productivity (Fig. 4B, C). *Trifarina fluens*, an indicator species of high productivity (e.g. Ślubowska-Woldengen *et al.* 2007), shows a peak in relative abundance right at the shift from a predominantly calcareous fauna to an agglutinated fauna (Figs 4B, C, G, 5J). The planktic foraminifera disappear entirely, while calcareous benthic specimens become very rare indicating almost complete dissolution of the calcareous fauna (Fig. 4B, C, G, Table S2). The higher organic supply to the sediment from seasonally open conditions could have caused

higher acidity in the sediment resulting in dissolution and fragmentation (cf. Steinsund & Hald 1994; Wollenburg *et al.* 2001).

Dominance of *E. clavatum*, together with *C. reniforme* and/or agglutinated species (Figs 4G, 5B, C) indicates cold polar conditions at the sea floor (Jennings & Helgadottir 1994). Holocene sediments from low-salinity conditions in the Arctic are dominated by *E. clavatum* and *C. reniforme* (no or few *C. neoteretis*) as for example in the Nares Strait, northern Greenland (Georgiadis *et al.* 2020) and the central NE Greenland shelf at 79°N (core 73G; Pados-Dibattista *et al.* 2022) (Fig. 1A). In core PS1230 from the NE Greenland slope at 1249-m water depth (Fig. 1A), Bauch *et al.* (2001) also noted poorer preservation of foraminifera in the Early Holocene compared to the glacial period.

*Upper section 27–0 cm (Middle–Late Holocene c. 7.5 ka–Recent): cooling and weakening of Atlantic Water inflow and polar conditions.* – The concentration of foraminifera in this section is very low and diversity is minimal (Figs 4B, C, 5K). Agglutinated species dominate, reaching >95 to 100% of the fauna indicating strong dissolution of calcareous foraminifera (Fig. 4G). Due to the absence of an *in-situ* calcareous fauna, no <sup>14</sup>C dates could be obtained. The sediment is very fine grained without IRD (Figs 3E, 4A), and we interpret the sediment as deposited under very similar conditions as today with extensive sea ice cover and relatively cold bottom water (Fig. 1D).

Core 73G from the NE Greenland shelf (Fig. 1A) shows increasing percentages of agglutinated specimens from c. 7.5 ka, but calcareous species remain high with dominance of *E. clavatum* and *C. reniforme* and presence of highly opportunistic benthic species (e.g. *Stetsonia horvathi* and *Epistominella arctica*) (Pados-Dibattista *et al.* 2022). In core PS93/025–2 (Fig. 1A) from the central NE Greenland shelf, benthic and planktic foraminifera become very rare after 4.5 ka and % fragmentation high, indicating dissolution (Zehlich *et al.* 2020). On the slope of NE Greenland in core PS1230 (Fig. 1A), the last c. 7 ka experienced strong dissolution and low flux of planktic foraminifera (Bauch *et al.* 2001).

Shelf faunas from the Arctic Ocean and Baffin Bay of Polar low-salinity conditions with seasonally open water and increased productivity are characterized by deposition of fine sediments and tend to be dominated by agglutinating foraminiferal assemblages composed of the same species as in core 19G (Schroeder-Adams *et al.* 1990; Jackson *et al.* 2021). Thus, Middle–Late Holocene records from Polar environments are often dominated by agglutinating foraminifera, probably due to corrosive conditions at the bottom. Notably, the development over the East Greenland shelf appears quite similar to the development in Barrow Strait, Arctic Canada. In a core affected by Polar Water, planktic

foraminifera disappear and benthic foraminifera become sporadic after *c.* 7 ka, as sea ice cover increased (Pieńkowski *et al.* 2013). In a record from further east in the Barrow Strait, which is more affected by Atlantic Water, *C. reniforme* is the most abundant benthic foraminiferal species throughout the Holocene, while agglutinated species appear from *c.* 6.8 ka as the environmental conditions turned more polar (Pieńkowski *et al.* 2012). In northern Baffin Bay, conditions during the last *c.* 4500 years turned more corrosive with increased sea ice cover and seasonally open water (Jackson *et al.* 2021).

#### *Iceberg turbate and LGM: was the NE Greenland Ice Sheet at the shelf edge at 79.4°N?*

Arctic and polar marine records are often affected by intense iceberg scouring obliterating geomorphological features and disturbing the sedimentary records making it difficult to reconstruct and date ice-sheet extents from glacial maxima (Klages *et al.* 2017 and references therein). The scouring mixes the sediment creating iceberg turbates (Vorren *et al.* 1983). They are found widespread on formerly glaciated margins, seen as buried ‘till-like’ diamictos. On presently glaciated margins they are seen as fresh ploughmarks or as ploughmarks beneath a sediment drape (Belderson *et al.* 1973; Vorren *et al.* 1983; Lien *et al.* 1989; Solheim 1991; Dowdeswell *et al.* 1993, 1994; Zecchin *et al.* 2016; Nielsen & Kuipers 2018). Intense iceberg ploughing often occurs during glacial maxima and deglaciations and the outer shelf edge of NE Greenland is riddled with ploughmarks (Arndt *et al.* 2017) including our study area as the sub-bottom profiles indicate (Fig. 2A). Large ploughmarks from tabular and multi-keeled icebergs are also found in some of the large cross-shelf troughs on the shelf (Arndt *et al.* 2017; Olsen *et al.* 2020). The central East Greenland shelf at 69–72°N and at 75°N is so intensively reworked by iceberg scouring that the deposits resemble tills (Dowdeswell *et al.* 1994) but can be classified as an iceberg turbate (Streuff *et al.* 2022). Ploughing also takes place on the NE Greenland shelf today; however, in the shelf-edge inlet of core site 19G the reworked sediments are found buried below seemingly undisturbed sediments (Fig. 2), evidencing that ploughing has not been active during the Holocene, i.e. not since the late deglacial transition into the Holocene. The shelf-edge inlet is flanked by bank areas of shallower water depth (Fig. 2; Arndt *et al.* 2015), where icebergs with keel depth exceeding ~300 m will run aground and thus not reach the seabed within the inlet. Furthermore, Arndt *et al.* (2017) noted a lack of iceberg ploughing in the outer Westwind Trough, which has a similar water depth as the inlet (Fig. 1A, B). Icebergs coming from the north with keel depth exceeding 300 m have thus not entered the Westwind Trough since the ice stream retreated (Arndt *et al.* 2017). This is in line with our results of

cessation of ploughing from the late deglaciation–Early Holocene onwards.

The presence of a buried iceberg turbate dating from the LGM and early deglaciation with a rich and well-preserved Arctic planktic and benthic foraminiferal fauna and numerous macrofossils indicates, even though mixed by iceberg scouring, that this fauna must have lived during the glacial period (Figs 4–6). Although likely not entirely ‘*in situ*’, the faunas cannot have been moved far. Studies from recent disturbances of the seabed after iceberg scouring show that the sediments are rapidly recolonized after the event (e.g. Gutt *et al.* 1996; Conlan *et al.* 1998; Peck *et al.* 1999; Robinson *et al.* 2021). As mentioned above, the presence of well-preserved and abundant foraminiferal and delicate macrofossil faunas (Fig. 6) is also an indication that the origin of the deposit is not as a till, but as an ice-distal glaciomarine sediment that after deposition has been mixed by grounding icebergs.

Thus, our record of glaciomarine sediment from the outer shelf of NE Greenland close to 79.4°N is a clear indication that a grounded NE Greenland Ice Sheet did not reach to the shelf edge at our specific site during the LGM (Figs 1A, 6). In addition, the benthic foraminiferal fauna shows only low abundance of so-called ice-proximal species (e.g. *Elphidium clavatum*, *Elphidium hallandense*, *Elphidium* spp.; Korsun & Hald 2000) and instead shows a high relative abundance of Atlantic Water and current-related species (*C. neoteretis*, *C. lobatulus*, *A. gallowayi*, *C. reniforme*, *Buccella* spp.; see above) indicating ice-distal conditions at the core site (Fig. 5C, D, E, G).

Geomorphological studies have indicated that the Greenland Ice Sheet has advanced across the shelf in the past. For example, based on geophysical and geomorphological records showing presence of sediment lobes, sediment lenses and channels on the slope, Evans *et al.* (2009) suggested that the ice sheet reached to the shelf edge along the entire NE Greenland shelf during the LGM (Fig. 1A). In contrast, Arndt *et al.* (2017) suggested that the LGM ice sheet reached the shelf edge north of 79.30°N and in the southern part from 76–77°N, while the ice likely did not reach the shelf edge in the central sector 77–79.30°N, as they here found numerous ploughmarks from icebergs. Laberg *et al.* (2017) investigated a small area just south of 76°N and concluded that the ice here also reached to the shelf edge during the LGM. Geomorphological data from the central part of the NE Greenland shelf indicated that the ice edge could be found in this area, and it was suggested as the minimum extension of the LGM ice sheet (Evans *et al.* 2009; Winkelmann *et al.* 2010; see also Funder *et al.* 2011 and modelling results by Gowan *et al.* 2021; Fig. 1A).

Common to these studies is the lack of absolute dating to constrain the age of the sea-floor bedforms and thus the actual age of the glaciers forming these.

There is also neither a definite timing of when the ice sheet potentially reached the shelf edge nor of the ice retreat. It is assumed, based on presence of only a thin drape of probably Holocene sediments, or no drape at all, that the underlying morphological features (e.g. mega-scale glacial lineations, end moraine ridges, hummocky subglacial bedforms, acoustically transparent sediments interpreted as tills) are of young age, i.e. LGM and deglaciation. Absolute dates from core records on the NE Greenland shelf are few, mainly because of lack of dateable material (e.g. Olsen *et al.* 2020). So far, most  $^{14}\text{C}$  dates of marine sediments from the northern part of the NE Greenland shelf indicate Younger Dryas and Holocene ages (Notholt 1998; Evans *et al.* 2002; Syring *et al.* 2020a, b; Zehnich *et al.* 2020; Davies *et al.* 2022; Pados-Dibattista *et al.* 2022). A record from Kong Oscar Fjord (71.5°N), gave Early Holocene ages (mixed planktic and benthic foraminifera) above till (Notholt 1998). In Young Sound at 74–74.3°N, Holocene dates (molluscs) were also obtained (Eriksen 2018).

Given the ages of the iceberg-reworked deposits in core 19G from the shelf edge, we suggest that scouring occurred sometime after 17.5 ka probably during the early deglaciation and that it became reduced during the transition to the Early Holocene. Undisturbed late glacial and deglacial sediments on the slope of Northeast and East Greenland are relatively thin (e.g. Nam *et al.* 1995; Stein *et al.* 1996; Notholt 1998; Bauch *et al.* 2001; Telesiński *et al.* 2015; Gabrielsen 2017; Ezat *et al.* 2019). On the deep NE Greenland slope in the northern Fram Strait (cores JM06-16MC, HH12-948MC, HH12-946MC, PS93/031; Fig. 1A), the thin deglacial horizons are barren of calcareous foraminifera and in some records sediments of deglacial age are entirely missing (Zamelczyk *et al.* 2012; Ezat *et al.* 2021; Spielhagen & Mackensen 2021). This could indicate low melting rates and continued perennial to near-perennial sea ice cover over the shelf and slope of NE Greenland (Spielhagen & Mackensen 2021). It is thus possible that the deglaciation of the NE Greenland shelf (Polar sector of the Fram Strait) occurred later than in the east (Atlantic sector of the Fram Strait) and maybe only took hold from the Holocene transition onwards.

## Conclusions

We have studied gravity core DA17-NG-ST01-019G (core 19G) from the outer NE Greenland shelf near the shelf edge at 79.4°N. The purpose was to reconstruct the palaeoceanographic development and the intensity of flow of Atlantic Water, and the influence of the NE Greenland Ice Sheet and icebergs over the outer shelf.

AMS- $^{14}\text{C}$  dating of macrofossils and foraminifera shows that the 19G record dates from before the LGM

25.5 cal. ka to the Recent, which to our knowledge is the first record of dates beyond the late deglaciation and Holocene in glaciomarine sediments from the NE Greenland shelf. The entire record contained planktic and benthic foraminiferal assemblages typical for Arctic environments and living on the NE Greenland shelf today and during the Holocene. The results show that the strongest flow of subsurface Atlantic Water below near-perennial sea ice cover occurred around the LGM at 25–c. 17.5 ka. Presence of sessile bryozoans depending on strong bottom currents support this. Thus, the inflow of warm Atlantic Water was most likely almost as strong and at times stronger than today, which may be due to influx of Return Atlantic Water directly from the West Spitsbergen Current. The flow was still fairly strong during the Early Holocene but diminishing, and towards the end of the period, the closed sea ice cover may have opened and productivity increased. During the Middle–Late Holocene from c. 7.5 ka, cold Polar Water influenced the outer shelf and calcareous foraminifera were dissolved and mainly agglutinated species persisted.

The results also indicated that the sediment dating from the LGM most likely represents an iceberg turbate, where the sedimentary deposits have been mixed by iceberg ploughing, probably during the early deglaciation after 17.5 cal. ka. The sediment contained a rich well-preserved fauna of foraminifera and macro-invertebrates. The finding of macrofossils with dates spanning the entire LGM shows that the NE Greenland Ice Sheet did not reach the shelf edge at this northern site at 79.4°N.

*Acknowledgements.* – We thank the captain, crew and scientific party on board RV ‘Dana’. We warmly thank Søren Rysgaard, Arctic Climate Centre, Aarhus University and Jørgen Bendtsen, ClimateLab, Copenhagen, for the CTD data from the core location. We also wish to thank Trine Ravn-Jensen for composing the X-ray fluorescence data set, Mimi Oksman, then Aarhus University, now Geological Survey of Denmark and Greenland, Copenhagen, and Mériadec Le Pabic, Aarhus University for their assistance in opening and sampling of the core. We thank IHS Markt for granting an academic licence to the Kingdom seismic interpretation software for SeisLab Aarhus. We are also grateful to Jesper Olsen and Marie Kanstrup from the Aarhus AMS Centre, Aarhus University and to Mériadec Le Pabic for carrying out the  $^{14}\text{C}$  measurements. Finally, we thank the two reviewers Anne Jennings and an anonymous reviewer for their very constructive and helpful suggestions to improve the manuscript. The NorthGreen17 expedition was funded by the Danish Centre for Marine Research and the Natural Science and Engineering Research Council of Canada. The research was funded by the Danish Council for Independent Research (grant no. 7014-00113B G-Ice project and 0135-00165B (GreenShelf), both to MSS) with additional funding from the European Union’s Horizon 2020 research and innovation program under Grant Agreement No. 869383 (ECOTIP; MSS). The research also received support from the Research Council of Norway through its Centers of Excellence funding scheme, grant number 223259, and UiT the Arctic University of Norway, Tromsø, Norway (TLR). GEUS granted time for TN to join the NorthGreen2017 Expedition. The authors declare no conflict of interests.

*Author contributions.* – TLR wrote the manuscript draft, with all co-authors contributing data and figures, and to the discussions and editing.

## References

- Aagaard, K. & Carmack, E. C. 1989: The role of sea ice and other fresh water in the Arctic circulation. *Journal of Geophysical Research* 94 (C10), 14485–14498.
- Arndt, J. E., Jokat, W., Dorschel, B., Myklebust, R., Dowdeswell, J. A. & Evans, J. 2015: A new bathymetry of the Northeast Greenland continental shelf: constraints on glacial and other processes. *Geochemistry, Geophysics, Geosystems* 16, 3733–3753.
- Arndt, J. E., Jokat, W. & Dorschel, B. 2017: The last glaciation and deglaciation of the Northeast Greenland continental shelf revealed by hydro-acoustic data. *Quaternary Science Reviews* 160, 45–56.
- Bauch, H. A., Erlenkeuser, H., Spielhagen, R. F., Struck, U., Matthiessen, J., Thiede, J. & Heinemeier, J. 2001: A multiproxy reconstruction of the evolution of deep and surface waters in the subarctic Nordic seas over the last 30,000 yr. *Quaternary Science Reviews* 20, 659–678.
- Belderson, R. H., Kenyon, N. H. & Wilson, J. B. 1973: Iceberg ploughmarks in the Northeast Atlantic. *Palaeogeography, Palaeoclimatology, Palaeoecology* 13, 215–224.
- Bjørk, A. A., Kjær, K. H., Korsgaard, N. J., Khan, S. A., Kjeldsen, K. K., Andresen, C. S., Box, J. E., Larsen, N. K. & Funder, S. 2012: An aerial view of climate-related glacier fluctuations in Southeast Greenland. *Nature Geoscience* 5, 427–432.
- Cage, A. G., Pieńkowski, A. J., Jennings, A., Knudsen, K. L. & Seidenkrantz, M.-S. 2021: Comparative analysis of six common foraminiferal species of the genera *Cassidulina*, *Paracassidulina*, and *Islandiella* from the Arctic-North Atlantic domain. *Journal of Micropalaeontology* 40, 37–60.
- Carstens, J., Hebbeln, D. & Wefer, G. 1997: Distribution of planktic foraminifera at the ice margin in the Arctic (Fram Strait). *Marine Micropalaeontology* 29, 257–269.
- Conlan, K. E., Lenihan, H. S., Kvitek, R. G. & Oliver, J. S. 1998: Ice scour disturbance to benthic communities in the Canadian high Arctic. *Marine Ecology Progress Series* 166, 1–16.
- Davies, J., Mathiasen, A. M., Kristiansen, K., Hansen, K. E., Wacker, L., Alstrup, A. K. O., Munk, O., Pearce, C. & Seidenkrantz, M.-S. 2022: Holocene ocean conditions off the Zachariae Isstrøm, Northeast Greenland. *Quaternary Science Reviews* 107530, 1–19.
- De Steur, L., Hansen, E., Gerdes, R., Karcher, M., Farbach, E. & Holfort, J. 2009: Freshwater fluxes in the East Greenland current: a decade of observations. *Geophysical Research Letters* 36, L23611, <https://doi.org/10.1029/2009GL041278>.
- Dowdeswell, J. A., Villinger, H., Whittington, R. J. & Marienfeld, P. 1993: Iceberg scouring in Scoresby Sund and on the East Greenland continental shelf. *Marine Geology* 111, 37–53.
- Dowdeswell, J. A., Whittington, R. J. & Marienfeld, P. 1994: The origin of massive diamictic facies by iceberg rafting and scouring, Scoresby Sund, East Greenland. *Sedimentology* 41, 21–35.
- El bani Altuna, N., Rasmussen, T. L., Ezat, M. M., Vadakkepulyambatta, S., Groeneveld, J. & Greaves, M. 2021a: Deglacial bottom water warming intensified Arctic methane seepage in the NW Barents Sea. *Communications Earth & Environment* 2, 188, <https://doi.org/10.1038/s43247-021-00264-x>.
- El bani Altuna, N., Ezat, M. M., Greaves, M. & Rasmussen, T. L. 2021b: Glacial millennial-scale changes in bottom water temperature and water mass exchange through the Fram Strait 79°N, 63–13 kyr. *Paleoceanography and Paleoclimatology* 36, e2020PA004061, <https://doi.org/10.1029/2020PA004061>.
- Eriksen, L. N. 2018: *Palaeoceanographic and climatic development of the NE Greenland shelf region and its impact on sediment deposition*. Master Thesis, Aarhus University, 159 pp.
- Evans, J., Dowdeswell, J. A., Grobe, H., Niessen, F., Stein, R., Hubberten, H. W. & Whittington, R. J. 2002: Late quaternary sedimentation in Kejsers Franz Joseph Fjord and the continental margin of East Greenland. *Geological Society Special Publication* 203, 149–179.
- Evans, J., Ó Cofaigh, C., Dowdeswell, J. A. & Wadhams, P. 2009: Marine geophysical evidence for former expansion and flow of the Greenland ice sheet across the north-East Greenland continental shelf. *Journal of Quaternary Science* 24, 279–293.
- Ezat, M. M., Rasmussen, T. L., Hain, M. P., Greaves, M., James, W. B., Rae, J. W. B., Zamelczyk, K., Marchitto, T. M., Szidat, S. & Skinner, L. C. 2021: Deep ocean storage of heat and CO<sub>2</sub> in the Fram Strait, Arctic Ocean during the last glacial period. *Paleoceanography and Paleoclimatology* 36, e2021PA004216, <https://doi.org/10.1029/2021PA004216>.
- Ezat, M., Rasmussen, T. L., Skinner, L. C. & Zamelczyk, K. 2019: Deep ocean <sup>14</sup>C ventilation age reconstructions from the Arctic Mediterranean reassessed. *Earth and Planetary Science Letters* 518, 67–75.
- Funder, S., Kjeldsen, K. K., Kjær, K. H. & Ó Cofaigh, C. 2011: The Greenland ice sheet during the past 300,000 years: a review. *Developments in Quaternary Science* 15, 699–713.
- Gabrielsen, L. 2017. *Study of millennial scale Paleoclimatic and Paleooceanographic changes in conjunction with variations in the East Greenland current during the late Quaternary*. Master thesis, UiT the Arctic University of Norway, 155 pp.
- Georgiadis, E., Giraudeau, J., Jennings, A., Limoges, A., Jackson, R., Ribeiro, S. & Massé, G. 2020: Local and regional control on Holocene Sea ice dynamics and oceanography in Nares Strait, Northwest Greenland. *Marine Geology* 422, 106125, <https://doi.org/10.1016/j.margeo.2020.106115>.
- Gowan, E. J., Zhang, X., Khosravi, S., Rovere, A., Stocchi, P., Hughes, A. L. C., Gyllenkretz, R., Mangerud, J., Svendsen, J. -I. & Lohmann, G. 2021: A new global ice sheet reconstruction for the past 80 000 years. *Nature Communications* 12, 1199, <https://doi.org/10.1038/s41467-021-21469-w>.
- Gutt, J., Starmans, A. & Dieckmann, G. 1996: Impact of iceberg scouring on polar benthic habitats. *Marine Ecology Progress Series* 137, 311–316.
- Hald, M. & Korsun, S. 1997: Distribution of modern benthic foraminifera from fjords of Svalbard, European Arctic. *Journal of Foraminiferal Research* 27, 101–122.
- Hald, M. & Steinsund, P. I. 1992: Distribution of surface sediment benthic foraminifera in the southwestern Barents Sea. *Journal of Foraminiferal Research* 22, 347–362.
- Hald, M., Sættem, J. & Nesse, E. 1990: Middle and late Weichselian stratigraphy in shallow drillings from the southwestern Barents Sea: foraminiferal, amino acid and radiocarbon evidence. *Norsk Geologisk Tidsskrift* 70, 241–257.
- Holland, D. M., Thomas, R. H., de Young, B., Ribergaard, M. H. & Lyberth, B. 2008: Acceleration of Jacobshavn Isbræ triggered by warm subsurface ocean waters. *Nature Geoscience* 1, 659–664.
- Hopkins, T. S. 1991: The GIN Sea – A synthesis of its physical oceanography and literature review 1972–1985. *Earth-Science Reviews* 30, 175–318.
- Howat, I. M., Joughin, I. & Scambos, T. A. 2007: Rapid changes in ice discharge from Greenland outlet glaciers. *Science* 315, 1559–1561.
- Jackson, R., Kvorning, A. B., Limoges, A., Georgiadis, E., Olsen, S. M., Tallberg, P., Andersen, T. J., Mikkelsen, N., Giraudeau, J., Massé, G., Wacker, L. & Ribeiro, S. 2021: Holocene polynya dynamics and their interaction with oceanic heat transport in northernmost Baffin Bay. *Scientific Reports* 11, 10095, <https://doi.org/10.1038/s41598-021-88517-9>.
- Jakobsson, M., Mayer, L., Coakley, B., Dowdeswell, J. A., Forbes, S., Fridman, B., Hodnesdal, H., Noormets, R., Pedersen, R., Rebesco, M., Schenke, H. W., Zarayskaya, Y., Accettella, D., Armstrong, A., Anderson, R. M., Bienhoff, P., Camerlenghi, A., Church, I., Edwards, M., Gardner, J. V., Hall, J. K., Hell, B., Hestvik, O., Kristoffersen, Y., Marcussen, C., Mohammad, R., Mosher, D., Nghiem, S. V., Pedrosa, M. T., Travaglini, P. G. & Weatherall, P. 2012: The International Bathymetric Chart of the Arctic Ocean (IBCAO) version 3.0. *Geophysical Research Letters* 39, L12609, <https://doi.org/10.1029/2012GL052219>.
- Jakobsson, M. and 51 others 2020: The International Bathymetric Chart of the Arctic Ocean Version 4.0. *Scientific Data* 7, 176, <https://doi.org/10.1038/s41597-020-0520-9>.
- Jennings, A. E. & Helgadottir, G. 1994: Foraminiferal assemblages from the fjords and shelf of eastern Greenland. *Journal of Foraminiferal Research* 24, 123–144.

- Jennings, A. E. & Weiner, N. J. 1996: Greenland during the last 1300 years: evidence from foraminifera and lithofacies in Nansen Fjord, 68°N. *The Holocene* 6, 179–191.
- Jennings, A. E., Andrews, J. & Wilson, L. 2011: Holocene environmental evolution of the SE Greenland shelf north and south of the Denmark Strait: Irminger and East Greenland current interactions. *Quaternary Science Reviews* 20, 980–998.
- Jennings, A. E., Knudsen, K. L., Hald, M., Hansen, C. V. & Andrews, J. T. 2002: A mid-Holocene shift in Arctic Sea-ice variability on the East Greenland shelf. *The Holocene* 12, 49–58.
- Johnsen, S. J., Clausen, H. B., Dansgaard, W., Fuhrer, K., Gundestrup, N., Hammer, C. U., Iversen, P., Jouzel, J., Stauffer, B. & Steffensen, J. P. 1992: Irregular glacial interstadials in a new Greenland ice core. *Nature* 359, 311–313.
- Khan, S. A., Björk, A. A., Bamber, J. L., Morlighem, M., Bevis, M., Kjær, K. H., Mouginot, J., Løkkegaard, A., Holland, D. M., Aschwanden, A., Zhang, B., Helm, V., Korsgaard, N. J., Colgan, W., Larsen, N. K., Liu, L., Hansen, K., Barletta, V., Dahl-Jensen, T. S., Søndergaard, A. S., Csatho, B. M., Sasgen, I., Box, J. & Schenk, T. 2020: Centennial response of Greenland's three largest outlet glaciers. *Nature Communications* 11, 5718, <https://doi.org/10.1038/s41467-020-19580-5>.
- Kjeldsen, K. K., Korsgaard, N. J., Björk, A. A., Khan, S. A., Box, J. E., Funder, S., Larsen, N. K., Bamber, J. L., Colgan, W., van den Broeke, M., Siggaard Andersen, M.-L., Nuth, C., Schomacker, A., Andresen, C. S., Willerslev, E. & Kjær, K. 2015: Spatial and temporal distribution of mass loss from the Greenland ice sheet since AD 1900. *Nature* 528, 396–400.
- Klages, J. P., Kuhn, G., Hillenbrand, C.-D., Smith, J. A., Graham, A. G. C., Nitsche, F. O., Frederichs, T., Jernas, P. E., Gohl, K. & Wacker, L. 2017: Limited grounding-line advance onto the West Antarctic continental shelf in the easternmost Amundsen Sea embayment during the last glacial period. *PLoS ONE* 12, e0181593, <https://doi.org/10.1371/journal.pone.0181593>.
- Kohfeld, K. E., Fairbanks, R. G., Smith, S. L. & Walsh, I. D. 1996: *Neogloboquadrina pachyderma* (sinistral coiling) as paleoceanographic tracers in polar oceans: evidence from northeast water polynya plankton tows, sediment traps, and surface sediments. *Paleoceanography* 11, 679–699.
- Korsun, S. & Hald, M. 2000: Seasonal dynamics of benthic foraminifera in a glacially fed fjord of Svalbard, European Arctic. *Journal of Foraminiferal Research* 30, 251–271.
- Kuklinski, P. & Bader, B. 2007: Diversity, structure and interactions of encrusting lithophilic macrofaunal assemblages from Belgica Bank, East Greenland. *Polar Biology* 30, 709–717.
- Laberg, J. S., Forwick, M. & Husum, K. 2017: New geophysical evidence for a revised maximum position of part of the NE sector of the Greenland ice sheet during the last glacial maximum. *Arktos* 3, 1–10. <https://doi.org/10.1007/s41063-017-0029-4>.
- Lien, R., Solheim, A., Elverhøi, A. & Rokoengen, K. 1989: Iceberg scouring and sea bed morphology on the eastern Weddell Sea shelf, Antarctica. *Polar Research* 7, 43–57.
- Lindemann, M. R., Straneo, F., Wilson, N. J., Toole, J. M., Krishfield, R. A., Beaird, N. L., Kansow, T. & Schaffer, J. 2020: Ocean circulation and variability beneath Nioghalvfjærdbræ (79 north glacier) ice tongue. *Journal of Geophysical Research Oceans* 125, e2020JC016091, <https://doi.org/10.1029/2020JC016091>.
- Lisiecki, L. E. & Raymo, M. E. 2005: A Pliocene-Pleistocene stack of 57 globally distributed benthic  $\delta^{18}\text{O}$  records. *Paleoceanography* 20, PA1003, <https://doi.org/10.1029/2004PA001071>.
- Lubinski, D. J., Polyak, L. & Forman, S. L. 2001: Freshwater and Atlantic water inflows to the deep northern Barents and Kara seas since ca 13  $^{14}\text{C}$  ka: foraminifera and stable isotopes. *Quaternary Science Reviews* 20, 1851–1879.
- Luckman, A., Murray, T., de Lange, R. & Hanna, E. 2006: Rapid and synchronous ice-dynamic changes in East Greenland. *Geophysical Research Letters* 33, L03503, <https://doi.org/10.1029/2005GL025428>.
- Löwemark, L. & Itrax operators (Bloemsmas, M., Croudace, I., Daly, J. S., Edwards, R. J., Francus, P., Galloway, J. M., Gregory, B. R. B., Huang, J.-J. S., Jones, A. F., Kylander, M., Löwemark, L., Luo, Y., Maclachlan, S., Ohlendorf, C., Patterson, R. T., Pearce, C., Profe, J., Reinhardt, E. G., Stranne, C., Tjallingii, R. & Turner, J. N.) 2019: Practical guidelines and recent advances in the Itrax XRF core-scanning procedure. *Quaternary International* 514, 16–29.
- Mankoff, K. D., Fettweis, X., Langen, P. L., Stendel, M., Kjeldsen, K. K., Karlsson, N. B., Noël, B., van den Broeke, M. R., Solgaard, A., Colgan, W., Box, J. E., Simonsen, S. B., King, M. D., Ahlström, A. P., Andersen, S. B. & Fausto, R. S. 2021: Greenland ice sheet mass balance from 1840 through next week. *Earth System Science Data* 13, 5001–5025.
- Mouginot, J., Rignot, E., Björk, A. A., van den Broeke, M., Millan, R., Morlighem, M., Noël, B., Scheuchl, B. & Wood, M. 2019: Forty-six years of Greenland ice sheet mass balance from 1972 to 2018. *Proceedings of the National Academy of Sciences* 116, 9239–9244, <https://doi.org/10.1073/pnas.1904242116>.
- Mouginot, J., Rignot, E., Scheuchl, B., Fenty, I., Khazendar, A., Morlighem, M., Buzzi, A. & Paden, J. 2015: Fast retreat of Zachariae Isstrøm, Northeast Greenland. *Science* 350, 1357–1361.
- Müller, J. & Stein, R. 2014: High-resolution record of late glacial and deglacial sea ice changes in Fram Strait corroborates ice-ocean interactions during abrupt climate shifts. *Earth and Planetary Science Letters* 403, 446–466.
- Nam, S. I., Stein, R., Grobe, H. & Hubberten, H. 1995: Late quaternary glacial-interglacial changes in sediment composition at the East Greenland continental margin and their paleoceanographic implications. *Marine Geology* 122, 243–262.
- Newton, A. C. & Rowe, G. T. 1995: The abundance of benthic calcareous foraminifera and other meiofauna at a time series station in the northeast water polynya, Greenland. *Journal of Geophysical Research* 100 (C3), 4423–4438.
- Nielsen, T. & Kuijpers, A. 2018: Glacially influenced morphodynamic features – examples from the north Faroe margin. *Marine Geology* 402, 131–138.
- Notholt, H. 1998: Die Auswirkungen der “Northeast Water” -Polynya auf die Sedimentation von NO-Grönland und Untersuchungen zur Paläo-Ozeanographie seit dem Mittelweichsel. *Berichte Polarforschung* 275, p. 196.
- Olsen, I. L., Rydningen, T. A., Forwick, M., Laberg, J. S. & Husum, K. 2020: Last glacial ice sheet dynamics offshore NE Greenland – a case study from store Koldewey trough. *The Cryosphere* 14, 4475–4494.
- Pados, T. & Spielhagen, R. F. 2014: Species distribution and depth habitat of recent planktic foraminifera in Fram Strait, Arctic Ocean. *Polar Research* 33, 22483, <https://doi.org/10.3402/polar.v33.22483>.
- Pados-Dibattista, T., Pearce, C., Detlef, H., Bendtsen, J. & Seidenkrantz, M. -S. 2022: Holocene paleoceanography of the Northeast Greenland shelf. *Climate of the Past* 18, 103–127.
- Peck, L. S., Brockington, S., Vanhove, S. & Beghyn, M. 1999: Community recovery following catastrophic iceberg impacts in a soft-sediment shallow-water site at Signy Island, Antarctica. *Marine Ecology Progress Series* 186, 1–8.
- Perner, K., Moros, M., Lloyd, J. M., Jansen, E. & Stein, R. 2015: Mid to late Holocene strengthening of the East Greenland current linked to warm subsurface Atlantic water. *Quaternary Science Reviews* 129, 296–307.
- Pieńkowski, A. J., England, J. H., Furze, M. F. A., Blasco, S., Mudie, P. J. & MacLean, B. 2013: 11,000 yrs of environmental change in the Northwest Passage: a multiproxy core record from central Parry Channel, Canadian high Arctic. *Marine Geology* 341, 68–85.
- Pieńkowski, A. J., England, J. H., Furze, M. F. A., Marret, F., Eynaud, F., Vilks, G., MacLean, B., Blasco, S. & Scourse, J. D. 2012: The deglacial to postglacial marine environments of SE Barrow Strait, Canadian Arctic Archipelago. *Boreas* 41, 141–179.
- Rasmussen, T. L., Thomsen, E., Ślubowska, M. A., Jessen, S., Solheim, A. & Koç, N. 2007: Paleoclimatological evolution of the SW Svalbard margin (76°N) since 20,000  $^{14}\text{C}$  yr BP. *Quaternary Research* 67, 100–114.
- Reimer, P. J., Edouard, B., Bayliss, A., Beck, J. W., Blackwell, P. G., Ramsey, C. B., Buck, C. E., Cheng, H., Edwards, R. L., Friedrich, M., Grootes, P. M., Guilderson, T. P., Hafllidason, H., Hajdas, I., Hatté, C., Heaton, T. J., Hoffmann, D. L., Hogg, A. G., Hughen, K. A., Kaiser, K. F., Kromer, B., Manning, S. W., Nju, M., Reimer, R. W., Richards, D. A., Scott, E. M., Southon, J. R., Staff, R. A., Turney, C.

- S. M. & van der Plicht, J. 2013: INTCAL13 and Marine13 radiocarbon age calibration curves 0–50,000 years cal BP. *Radiocarbon* 55, 1869–1886.
- Richter, T. O., Van der Gaast, S., Koster, B., Vaars, A., Gieles, R., de Stigter, H. C., de Haas, H. & van Weering, T. C. E. 2006: The Avaatech XRF Core scanner: technical description and applications to NE Atlantic sediments. *Geological Society Special Publications* 267, 39–50.
- Rignot, E. & Mouginot, J. 2012: Ice flow in Greenland for the international polar year 2008–2009. *Geophysical Research Letters* 39, L11501, <https://doi.org/10.1029/2012GL051634>.
- Robinson, B. J. O., Barnes, D. K. A., Grange, L. J. & Morley, S. A. 2021: Intermediate ice scour disturbance is key to maintaining a peak in biodiversity within the shallows of the Western Antarctic peninsula. *Scientific Reports* 11, 16712, <https://doi.org/10.1018/s41598-021-96769-9>.
- Rothwell, R. & Croudace, I. 2015: Twenty years of XRF core scanning marine sediments: what do geochemical proxies tell us? In Croudace, I. & Rothwell, R. (eds.): *Micro-XRF Studies of Sediment Cores. Developments in Paleoenvironmental Research* 17. Springer, Dordrecht, [https://doi.org/10.1007/978-94-017-9849-5\\_2](https://doi.org/10.1007/978-94-017-9849-5_2).
- Rudels, B., Björk, G., Nilsson, J., Winsor, P., Lake, I. & Nohr, C. 2005: The interaction between waters from the Arctic Ocean and the Nordic seas north of Fram Strait and along the East Greenland current: results from the Arctic Ocean-02 expedition. *Journal of Marine Systems* 55, 1–30.
- Rudels, B., Fahrback, E., Meincke, J., Budéus, G. & Eriksson, P. 2002: The East Greenland current and its contribution to the Denmark Strait overflow. *ICES Journal of Marine Sciences* 59, 1133–1154.
- Schaffer, J., Kansow, T., von Appen, W.-J., von Albedyll, L., Arndt, J. E. & Roberts, D. H. 2020: Bathymetry constraints ocean heat supply to Greenland's largest glacier tongue. *Nature Geoscience* 13, 227–231.
- Schroeder-Adams, J. J., Cole, F. E., Mediol, F. S., Mudie, P. J., Scott, D. B. & Dobbins, L. 1990: Recent Arctic shelf foraminifera: seasonally ice covered vs. perennially ice covered areas. *Journal of Foraminiferal Research* 20, 8–36.
- Seidenkrantz, M.-S. 1995: *Cassidulina teretis* Tappan and *Cassidulina neoteretis* new species (foraminifera): stratigraphic markers for deep sea and outer shelf areas. *Journal of Micropalaeontology* 14, 145–157.
- Seidenkrantz, M.-S., Andersen, J. R., Andresen, K. J., Bendtsen, J., Brice, C., Ellegaard, M., Eriksen, L. N., Gariboldi, K., Le Duc, C., Mathiasen, A. M., Nielsen, T., Ofstad, S., Pearce, C., Rasmussen, T. L., Ribeiro, S., Rysgaard, S., Røy, H., Scholze, C., Schultz, M. & Wangner, D. J. 2018: *NorthGreen2017 - a Marine Research Expedition to NE Greenland Onboard 'R/V Dana' September 17 to October 1*. Cruise Report, Aarhus University, Aarhus, Denmark, 53 pp.
- Seidenkrantz, M.-S., Kuijpers, A., Aagaard-Sørensen, S., Lindgreen, H., Olsen, J. & Pearce, C. 2021: Evidence for influx of Atlantic water masses to the Labrador Sea during the Last Glacial Maximum. *Scientific Reports* 11, 6788, <https://doi.org/10.1038/s41598-021-86224-z>.
- Seidenkrantz, M.-S., Kuijpers, A., Olsen, J., Pearce, C., Lindblom, S., Ploug, J., Przybyło, P. & Snowball, I. 2019: Southwest Greenland shelf glaciation during MIS 4 more extensive than during the last glacial maximum. *Scientific Reports* 9, 15617, <https://doi.org/10.1038/s41598-019-51983-3>.
- Simonsen, S. B., Barletta, V. R., Colgan, W. T. & Sørensen, L. S. 2021: Greenland Ice Sheet mass balance (1992–2020) from calibrated radar altimetry. *Geophysical Research Letters* 48, e2020GL091216, <https://doi.org/10.1029/2020GL091216>.
- Solheim, A. 1991: The depositional environment of surging sub-polar tidewater glaciers. A case study of the morphology, sedimentation and sediment properties in a surge-affected marine basin outside Nordaustlandet, Northern Barents Sea. *Norwegian Polar Institute Skrifter no. 194*, 98 pp.
- Sørensen, M. 2012: Walrus Island – A pivotal place for high Arctic Palaeo-Eskimo societies in Northeast Greenland. *Études/Inuit Studies* 36, 183–205.
- Spielhagen, R. F. & Mackensen, A. 2021: Upper Ocean variability off NE Greenland (79°N) since the last glacial maximum reconstructed from stable isotopes in planktic foraminifer morphotypes. *Quaternary Science Reviews* 265, 107070, <https://doi.org/10.1016/j.quascirev.2021.107070>.
- Stein, R., Nam, S.-I., Grobe, H. & Hubberten, H. 1996: Late Quaternary glacial history and short-term ice-rafted debris fluctuations along the East Greenland continental margin. *Geological Society Special Publication* 111, 135–151.
- Steinsund, P. I. 1994: Benthic Foraminifera in Surface Sediments of the Barents and Kara Seas: Modern and Late Quaternary Applications. Ph.D. thesis, UiT the Arctic University of Norway, 111 pp.
- Steinsund, P. I. & Hald, M. 1994: Recent calcium carbonate dissolution in the Barents Sea: paleoceanographic implications. *Marine Geology* 117, 303–316.
- Streuff, K. K., Ó Cofaigh, C. & Wintersteller, P. 2022: GlaciDat – a GIS database of submarine glacial landforms and sediments in the Arctic. *Boreas*, <https://doi.org/10.1111/bor.12577>.
- Swift, J. H. 1986: *The Arctic waters*. In Hurdle, B. G. (ed.): *The Nordic Seas*, 129–154. Springer, New York.
- Syring, N., Lloyd, J. M., Stein, R., Fahl, K., Roberts, D. H., Callard, L. & Ó Cofaigh, C. 2020a: Holocene interactions between glacier retreat, sea ice formation, and Atlantic water advection at the inner Northeast Greenland continental shelf. *Paleoceanography and Paleoclimatology* 35, e2020PA004019, <https://doi.org/10.1029/2020PA004019>.
- Syring, N., Stein, R., Fahl, K., Vahlenkamp, M., Zehlich, M., Spielhagen, R. F. & Niessen, F. 2020b: Holocene changes in sea-ice cover and polynya formation along the eastern North Greenland shelf: new insights from biomarker records. *Quaternary Science Reviews* 231, 106173, <https://doi.org/10.1016/j.quascirev.2020.106173>.
- Ślubowska-Woldengen, M., Rasmussen, T. L., Koç, N., Klitgaard-Kristensen, D., Nilsen, F. & Solheim, A. 2007: Advection of Atlantic water to the western and northern Svalbard shelf since 17,500 cal yr BP. *Quaternary Science Reviews* 26, 463–478.
- Telesiński, M. M., Bauch, H. A., Spielhagen, R. F. & Kandiano, E. S. 2015: Evolution of the central Nordic seas over the last 20 thousand years. *Quaternary Science Reviews* 121, 98–109.
- Van den Broeke, M., Bamber, J., Ettema, J., Rignot, E., Schrama, E., van de Berg, W. J., van Meijgaard, E., Velicogna, I. & Wouters, B. 2009: Partitioning recent Greenland mass loss. *Science* 326, 984–986.
- Vasskog, K., Langebroek, P. M., Andrews, J. T., Nilsen, J. E. Ø. & Nesje, A. 2015: The Greenland ice sheet during the last glacial cycle: current ice loss and contribution to sea-level rise from a palaeoclimatic perspective. *Earth-Science Reviews* 150, 45–67.
- Vorren, T. O., Hald, M., Edvardsen, M. & Lind-Hansen, O. W. 1983: Glacigenic sediments and sedimentary environments on continental shelves: general principles with a case study from the Norwegian shelf. In Ehlers, J. (ed.): *Glacial Deposits in North-West Europe*, 61–73. Balkema, Rotterdam.
- Weinelt, M., Vogelsang, E., Kucera, M., Pflaumann, U., Sarnthein, M., Voelker, A., Erlenkeuser, H. & Malmgren, B. A. 2003: Variability of North Atlantic heat transfer during MIS 2. *Paleoceanography* 18, 1071.
- Wilken, M. & Mienert, J. 2006: Submarine glacigenic debris flows, deep-sea channels and past ice-stream behaviour of the East Greenland continental margin. *Quaternary Science Reviews* 25, 784–810.
- Winkelmann, D., Jokat, W., Jensen, L. & Schenke, H. -W. 2010: Submarine end moraines on the continental shelf off NE Greenland – implications for Lateglacial dynamics. *Quaternary Science Reviews* 29, 1069–1077.
- Wollenburg, J. E. & Mackensen, A. 1998: Living benthic foraminifers from the Central Arctic Ocean: faunal composition, standing stock and diversity. *Marine Micropaleontology* 34, 153–185.
- Wollenburg, J. E., Kuhnt, W. & Mackensen, A. 2001: Changes in Arctic Ocean paleoproductivity and hydrography during the last 145 kyr: the benthic foraminiferal record. *Paleoceanography* 16, 65–77.
- Zamani, B., Krumpfen, T., Smedsrud, L. H. & Gerdes, R. 2019: Fram Strait sea ice export affected by thinning: comparing high-resolution simulations and observations. *Climate Dynamics* 53, 3257–3270.
- Zamelczyk, K., Rasmussen, T. L., Husum, K., Haflidason, H., de Vernal, A., Ravna, E. K., Hald, M. & Hillaire-Marcel, C. 2012:

Between two oceanic fronts: paleoceanographic changes and calcium carbonate dissolution in the central Fram Strait during the last 20,000 years. *Quaternary Research* 78, 405–416.

Zecchin, M., Rebesco, M., Lucchi, R. G., Caffau, M., Lantsch, H. & Hanebuth, T. J. J. 2016: Buried iceberg-keel scouring on the southern Spitsbergenbanken, NW Barents Sea. *Marine Geology* 382, 68–79.

Zehnick, M., Spielhagen, R. F., Bauch, H. A., Forwick, M., Hass, H. C., Palme, T., Stein, R. & Syring, N. 2020: Environmental variability off NE Greenland (western Fram Strait) during the past 10,600 years. *The Holocene* 30, 1752–1766.

## Supporting Information

Additional Supporting Information to this article is available at <http://www.boreas.dk>.

*Table S1.* List of benthic foraminiferal species encountered in core DA17-NG-ST01-019G (19G) in alphabetical order.

*Table S2.* Data files with absolute abundances and percentage data of planktic and benthic foraminifera.

*Fig. S1* High-resolution figure of line scan and radiographic X-ray images of core 19G from measurements from the ITRAX core scanner as shown in Fig. 3 (see also main text for explanation).

*Fig. S2.* Calcareous polychaete tube of genus *Spirorbis* still attached to a dropstone.